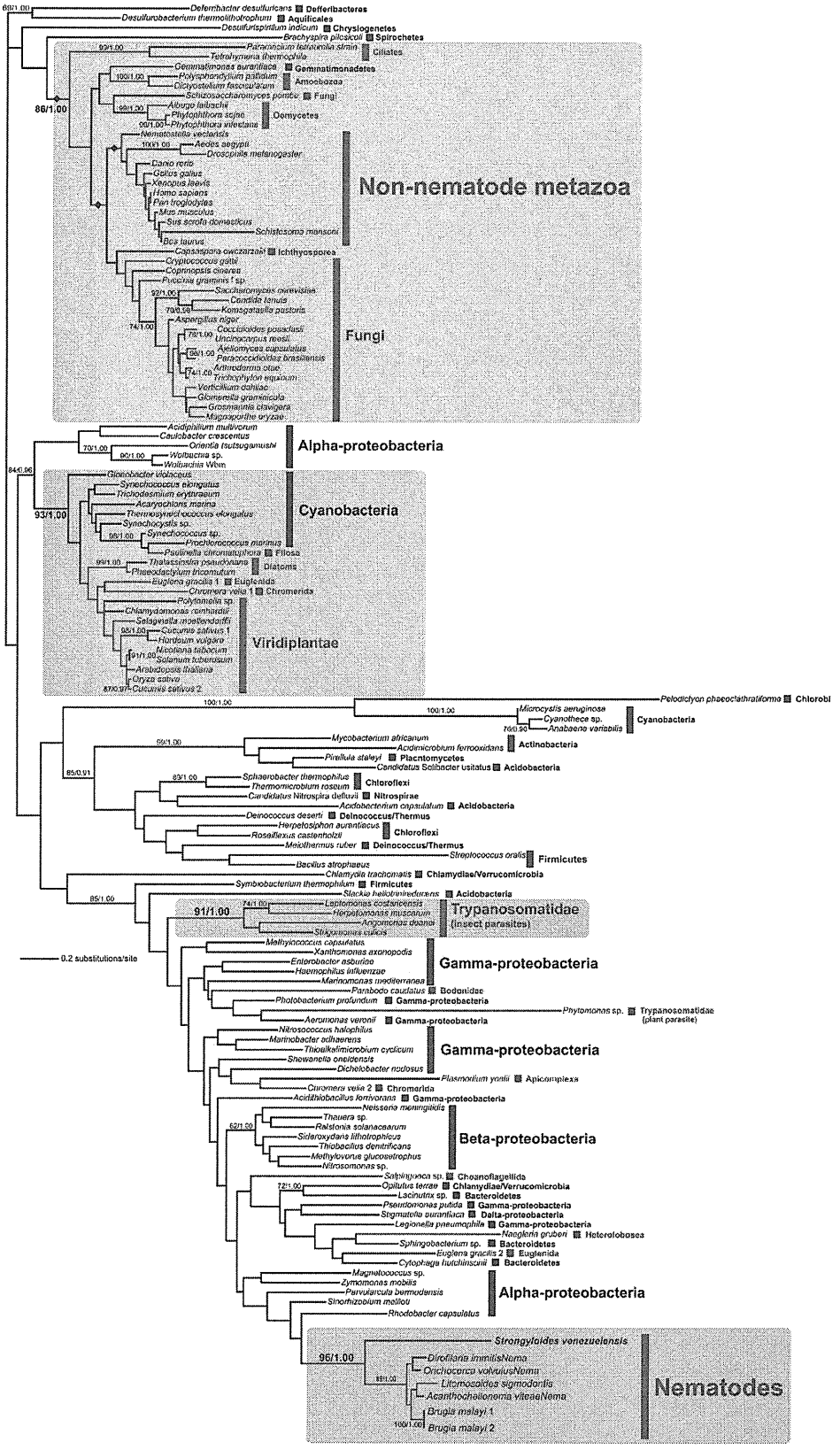
Deferribacter desulfuricans Deferribacteres
Desulfurobacterium thermolithotrophum Aquificales
Desulfurispirillum indicum Chrysiogenetes
Brachyspira pilosicoli Spirochetes
Paramecium tetraurelia strain Ciliates
Tetrahymena thermophila
Gemmatimonas aurantiaca Gemmatimonadetes
Polysphondylium pallidum
Dictyostelium fasciculatum Amoebozoa
Schizosaccharomyces pombe Fungi
Albugo laibachii
Phytophthora sojae Oomycetes
Phytophthora infestans
Nematostella vectensis
Aedes aegypti
Drosophila melanogaster
Danio rerio
Gallus gallus
Xenopus laevis
Homo sapiens
Pan troglodytes
Mus musculus
Sus scrofa domesticus
Schistosoma mansoni
Bos taurus
Capsaspora owczarzaki Ichthyosporea
Cryptococcus gattii
Coprinopsis cinerea
Puccinia graminis f sp.
Saccharomyces cerevisiae
Candida tenuis
Komagataella pastoris
Aspergillus niger
Coccidioides posadasii
Uncinocarpus reesii
Ajellomyces capsulatus
Paracoccidioides brasiliensis
Arthroderma otae
Trichophyton equinum
Verticillium dahliae
Glomerella graminicola
Grosmannia clavigera
Magnaporthe oryzae
Non-nematode metazoa
Fungi
Acidiphilium multivorum
Caulobacter crescentus
Orientia tsutsugamushi
Wolbachia sp.
Wolbachia Wbm
Alpha-proteobacteria
Gloeobacter violaceus
Synechococcus elongatus
Thermosynechococcus elongatus
Synechocystis sp.
Prochlorococcus marinus
Pseudanabaena chromatophora Filosa
Thalassiosira pseudonana Diatoms
Phaeodactylum tricornutum
Euglena gracilis 1 Euglenida
Chromera velia 1 Chromerida
Polytomella sp.
Chlamydomonas reinhardtii
Selaginella moellendorffii
Cucumis sativus 1
Hordeum vulgare
Nicotiana tabacum
Solanum tuberosum
Arabidopsis thaliana
Oryza sativa
Cucumis sativus 2
Cyanobacteria
Viridiplantae
Pelodictyon phaeoclathratiforme Chlorobi
Microcystis aeruginosa
Cyanothece sp.
Anabaena variabilis Cyanobacteria
Mycobacterium africanum
Acidimicrobium ferrooxidans Actinobacteria
Pirellula staleyi Planctomycetes
Candidatus Solibacter usitatus Acidobacteria
Sphaerobacter thermophilus
Thermomicrobium roseum Chloroflexi
Candidatus Nitrospira defluvii Nitrospirae
Acidobacterium capsulatum Acidobacteria
Deinococcus deserti Deinococcus/Thermus
Herpetosiphon aurantiacus
Roseiflexus castenholzii Chloroflexi
Meiothermus ruber Deinococcus/Thermus
Streptococcus oralis
Bacillus atrophaeus Firmicutes
Chlamydia trachomatis Chlamydiae/Verrucomicrobia
Symbiobacterium thermophilum Firmicutes
Stackia heliotrinireducens Acidobacteria
Leptomonas costaricensis
Herpetomonas muscarum
Angomonas deanei
Strigomonas culicis
Trypanosomatidae (insect parasites)
0.2 substitutions/site
Methylococcus capsulatus
Xanthomonas axonopodis
Enterobacter asburiae
Haemophilus influenzae
Marinomonas mediterranea
Paraboto caudatus Bodonidae
Photobacterium profundum Gamma-proteobacteria
Phytomonas sp. Trypanosomatidae (plant parasite)
Aeromonas veronii Gamma-proteobacteria
Gamma-proteobacteria
Nitrosococcus halophilus
Marinobacter adhaerens
Thioalkalimicrobium cyclicum
Shewanella oneidensis
Dichelobacter nodosus
Plasmodium yoelii Apicomplexa
Chromera velia 2 Chromerida
Acidithiobacillus ferrivorans Gamma-proteobacteria
Beta-proteobacteria
Neisseria meningitidis
Thauera sp.
Ralstonia solanacearum
Sideroxydans lithotrophicus
Thiobacillus denitrificans
Methylovorus glucosetrophus
Nitrosomonas sp.
Salpingoeca sp. Choanoflagellida
Opitutus terrae Chlamydiae/Verrucomicrobia
Lacinutrix sp. Bacteroidetes
Pseudomonas putida Gamma-proteobacteria
Stigmatella aurantiaca Delta-proteobacteria
Legionella pneumophila Gamma-proteobacteria
Naegleria gruberi Heterolobosea
Sphingobacterium sp. Bacteroidetes
Euglena gracilis 2 Euglenida
Cytophaga hutchinsonii Bacteroidetes
Magnetococcus sp.
Zymomonas mobilis
Parvularcula bermudensis
Sinorhizobium meliloti
Rhodobacter capsulatus
Alpha-proteobacteria
Strongyloides venezuelensis
Dirofilaria immitisNema
Onchocerca volvulusNema
Litomosoides sigmodontis
Acanthocheilonema viteaeNema
Brugia malayi 1
Brugia malayi 2
Nematodes

Figure 3. Phylogenetic analysis of FeCH sequences. The ML phylogeny inferred from FeCH amino acid sequences from 71 bacteria and 65 eukaryotes. Numerical values at the nodes represent MLBPs and BPPs. Only MLBPs greater than 60% are shown. The majority of the FeCH homologs sampled from eukaryotes (colored in red) were separated into four clades shaded in blue, green, pink, and orange. The homologs from *Strongyloides venezuelensis* identified in this study formed the 'orange' clade with those of other nematodes. We compared the ML tree and the alternative hypotheses for the origin of the nematode FeCH genes by pruning and regrafting the entire nematode clade (shaded in orange) to the branches marked by diamonds in the 'blue' clade.
doi:10.1371/journal.pone.0058458.g003

Tween 20, and 0.3 M NaCl. Cells were disrupted by sonication and centrifuged at 5000×g at 4°C for 10 min. The supernatants were used for the enzyme assay.

The FeCH activity was determined by measuring the insertion of zinc ions into mesoporphyrin, as described previously [42]. After incubation at 30°C for 30 min, the protoporphyrin or zinc-protoporphyrin formed was measured fluorophotometrically.

Genetic Complementation Assay of hemH (Bacterial FeCH) Deficient *E. coli*

E. coli strain VS200 (ΔhemH), a deletion mutant for hemH gene [43] was provided by the National Bioresource Project of MEXT, Japan.

The entire ORF of *Sv*FeCH, obtained by RT-PCR with the primer pair ENM089/ENM098, was cloned into the *Xho*I/*Bgl*II restriction site of pFLAG-CTC plasmid, an *E. coli* expression vector containing a tac promoter (Sigma-Aldrich, St. Louis, MO, USA). The resultant plasmid pFLAG-CTC-*Sv*FeCH was tested as a gene complementation vector. The original pFLAG-CTC plasmid served as a control.

ΔhemH was transformed with pFLAG-CTC-*Sv*FeCH or with pFLAG-CTC. The transformed and untransformed *E. coli* ΔhemH strains were cultured overnight in LB medium supplemented with hemin (10 μg/ml).

For the culture of the transformed ΔhemH, ampicillin was also added at a concentration of 50 μg/ml. The bacteria from the overnight culture were pelleted by centrifugation and washed thrice with LB medium. After washing, the bacteria pellets were resuspended to give an OD_{600} of 0.1 in hemin-containing (10 μg/ml) or hemin-free LB medium with (for the transformed ΔhemH) or without (for the untransformed ΔhemH) ampicillin, and incubated at 37°C with rocking. O.D. 600 of each culture was measured every hour up to 20 h.

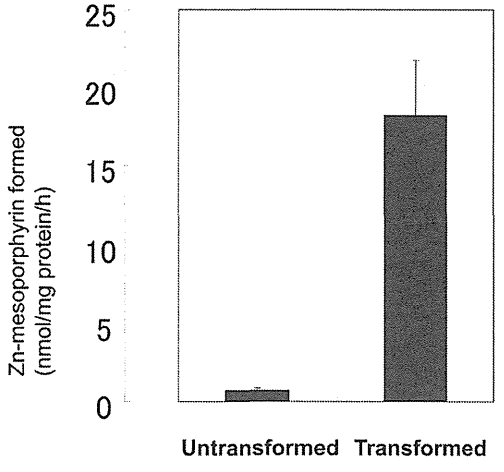

Figure 4. Chelatase assay using bacterially expressed recombinant *Sv*FeCH. The cell extracts were incubated with 20 mM Tris-HCl, pH 8.0, 0.1% Tween 20, 15 μM mesoporphyrin IX, and 40 μM zinc acetate in a final volume of 200 μl at 30°C for 60 min. The formation of zinc mesoporphyrin was measured. Data are expressed as the mean ± SD of triplicate experiments.
doi:10.1371/journal.pone.0058458.g004

Real-time RT-PCR Analysis

Total RNA samples were prepared from eggs, a mixture of first- and second-stage larvae (L1/L2), third-stage infective larvae (L3i), lung third-stage larvae (LL3), mucosal larvae (ML) and parasitic adult stages. Eggs were obtained by the floatation method with saturated salt solution from rat feces. L1/L2 and L3i were prepared from fecal culture. LL3 and ML were collected from infected male ICR mice 72 and 85 h after infection, respectively. Parasitic adults were collected from the small intestine of rats 10 days after infection. Eggs and worms were washed extensively with PBS, pelleted by centrifugation and stored at −80°C until used.

Frozen eggs or worms were crushed with a crushing device (SK-200) purchased from Tokken, Japan. Trizol (Invitrogen) was used for total RNA preparation following the manufacturer's instructions. After DNase I treatment, cDNA was synthesized using PrimeScript RT-PCR kit. Real-time RT-PCR was performed by the GoTaq qPCR system (***Promega***, Madison, WI, USA) using specific primer pairs (ENM056/ENM057 for *Sv*FeCH and 377F/501R for 18S ribosomal RNA genes). The real-time RT-PCR analyses were performed using biological triplicate samples.

Results

Initially, we identified an EST contig that appeared to represent a transcript from *Sv*FeCH gene [22]. The entire cDNA sequence was determined by 3′- and 5′- RACE experiments. This sequence could be mapped to the genomic DNA sequence of this organism obtained from our genome sequencing project, the details of which will be published elsewhere. The genomic and cDNA sequences of the *Sv*FeCH gene are presented in Figure 1. The length of the coding region was 1122 bp including the stop codon. There was one short (49 bp) intron. The deduced amino acid sequence had a length of 373 residues and an expected molecular mass of 43.3 kDa.

In our search for the presence of other heme biosynthesis genes, BLAST homology searches were performed against nematode genome and EST databases, using human heme biosynthesis gene sequences as queries (Tables S3 and S4). Overall, many nematodes appeared to lack all the heme biosynthesis genes, as reported for *C. elegans* [13]. However, some exceptions were also noticed, including the presence of the aminolevulinic acid dehydrogenase (ALAD) gene in several species and the uroporphyrinogen decarboxylase (UROD) gene in *Meloidogyne paranaensis*, the coproporphyrinogen oxidase (CPOX) gene in *Ancylostoma caninum*, and the FeCH gene in *B. malayi* and *Strongyloides ratti*. No heme biosynthesis gene other than FeCH was found in our *S. venezuelensis* genome and transcriptome data using the human sequences as queries. We did not obtain any significant hit from the BLAST analyses for *S. venezuelensis* genome and transcriptome datasets using the ALAD, UROD, and CPOX gene sequences identified in the nematode genome/EST datasets (see above) as queries. When the *Sv*FeCH protein sequence was used as a query for the BLAST analysis, two additional species were found to carry FeCH gene

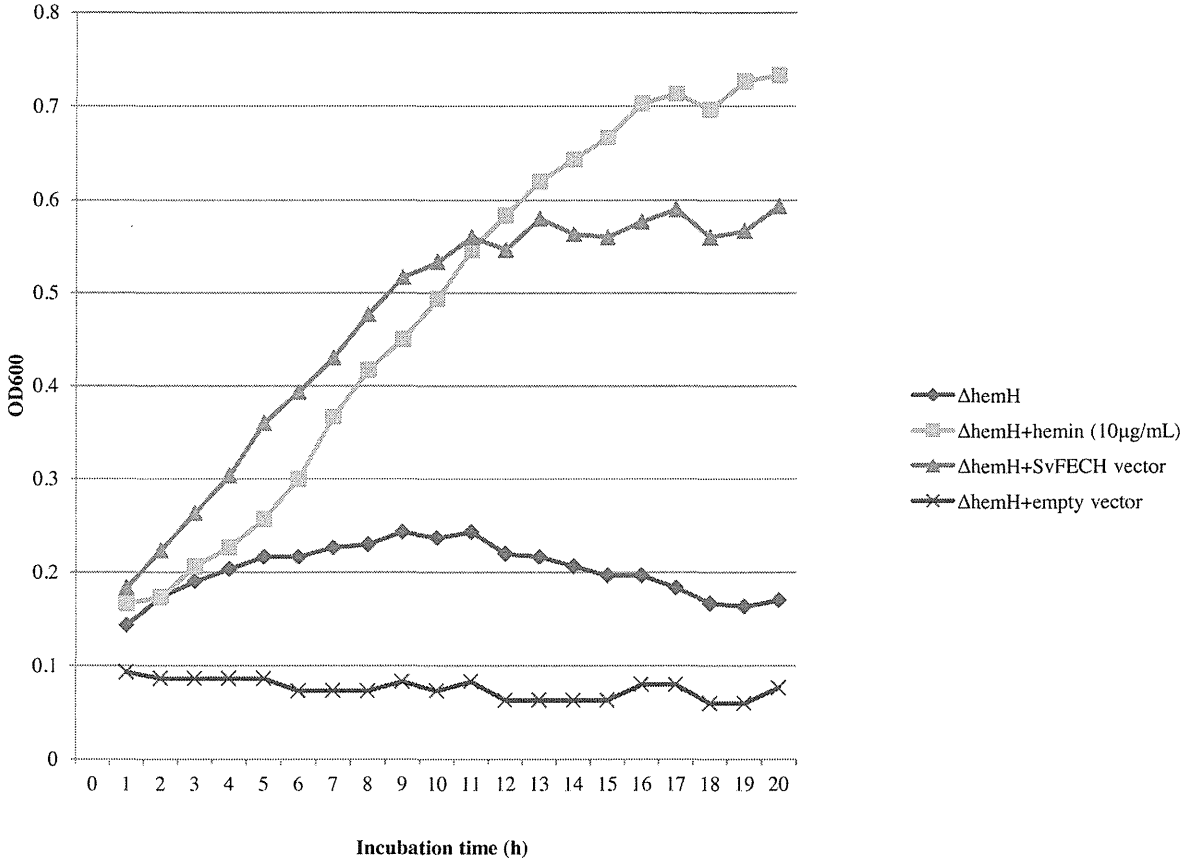

Figure 5. Genetic complementation assay of ΔhemH *E. coli*. An untransformed ΔhemH strain of *E. coli* was grown in the absence (diamond) or presence 10 μg/ml hemin (square). In the same experiment, a transformed ΔhemH strain of *E. coli* either with *Sv*FeCH gene expression vector (triangle) or with empty vector (x-mark) was cultured in the absence of hemin. OD_{600} was measured every hour up to 20 h to monitor bacterial growth.
doi:10.1371/journal.pone.0058458.g005

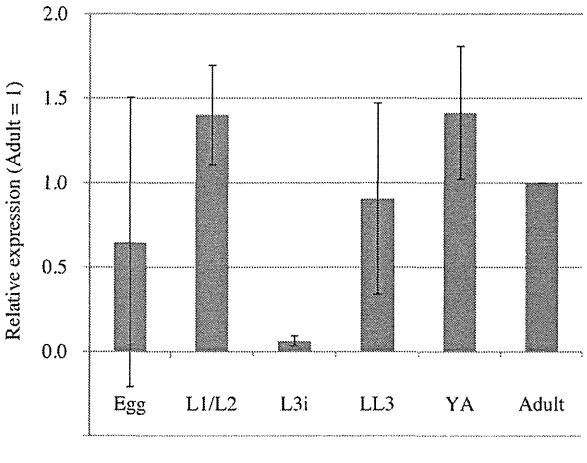

Figure 6. Expression analysis of *Sv*FeCH gene by real-time RT-PCR. mRNA abundance is shown ***relative*** to the expression level at the adult stage, after normalizing to 18S rRNA expression levels. The bars represent the means and standard deviations (±) of biological triplicates. Real-time RT-PCR was performed in triplicate wells for each biological replicate.
doi:10.1371/journal.pone.0058458.g006

(Table S5), namely *Litomosoides sigmodontis* and *Onchocerca volvulus*. The *S. venezuelensis* sequence was also used for BLAST searches against NCBI non-redundant protein database, which led to the identification of two more nematode species that carry FeCH, namely *Dirofilaria immitis* and *Acanthocheilonema viteae*. These results are interesting because all the species found to carry the FeCH gene were animal parasites (filarial nematodes in clade III and *Strongyloides* in clade IV).

A multiple sequence alignment of FeCH protein sequences from selected organisms is presented in Figure 2. Amino acid residues in the catalytic core (boxed by a red dotted line) displayed moderate similarity. Key residues for FeCH activity, such as H263 (human sequence numbering), which was proposed to be involved in metal substrate binding [23,44], were well conserved. Characteristically, nematode (*S. venezuelensis* and *B. malayi*) FeCH lacked a protein region called the "C-terminal extension," a short (approximately 30–50 amino acid residues) stretch of sequences at the C-terminus of the protein that is commonly present in the FeCH of non-nematode opisthokonts [23,45] (boxed by a green dotted line in Figure 2). To measure the similarities of these selected sequences, BLAST scores and amino acid identities were retrieved by the BLASTP program (Table S6). All the nematode FeCH sequences had higher BLAST scores and percent similarity values to the *E. coli* sequence (BLAST score: 202–221; similarity: 33.6%–36.8%)

a)

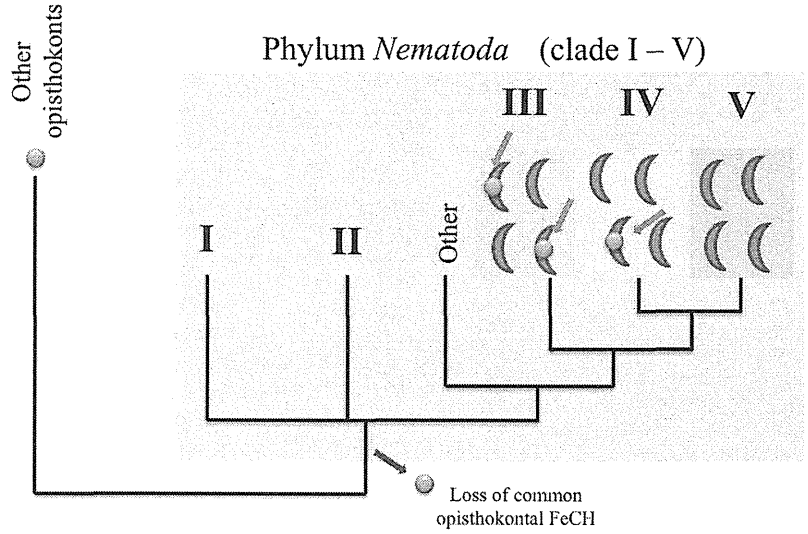

b)

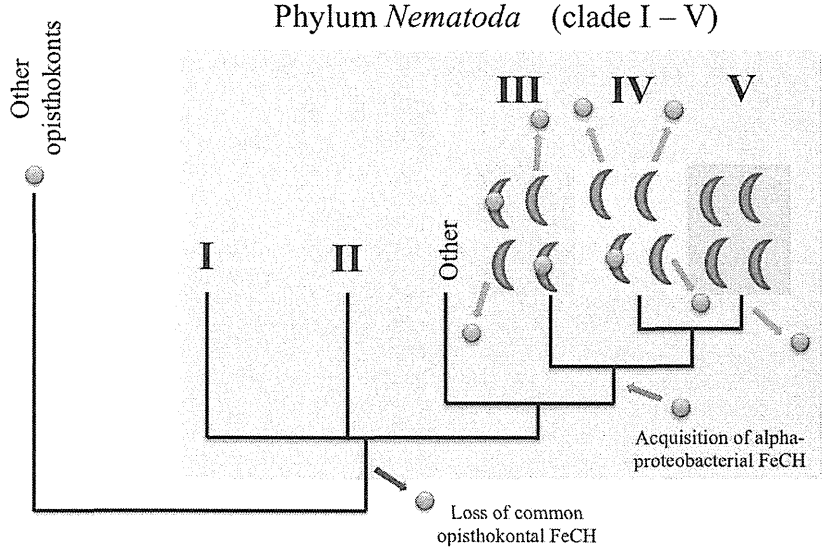

FeCH gene (common opisthokontal)

FeCH gene (alpha-proteobacterial)

Figure 7. Proposed hypotheses for the loss of the original (common opisthokontal) FeCH gene and the re-acquisition of alpha-proteobacterial FeCH in the evolution of the phylum Nematoda. The initial loss of the common opisthokontal FeCH gene may have occurred at the common ancestor level (red arrows). (a) Scenario 1: The first scenario hypothesizes that alpha-proteobacterial FeCH was acquired independently by some species in clades III and IV (green arrows). b) Scenario 2: Reacquisition of FeCH from an alpha-proteobacterium may have occurred at the common ancestor level of clades III, IV and V (blue arrow) followed by a secondary loss in some species in clade III and IV and in the branch leading to clade V (pink arrows). The phylogenetic relationships of the nematode clades are based on Sommer and Streit [10].
doi:10.1371/journal.pone.0058458.g007

than to human (92–106 and 26.8%–27.5%, respectively), *Drosophila* (93–102 and 24.0%–25.9%, respectively) and *Saccharomyces* sequences (74–96 and 23.0%–27.2%, respectively). When BLAST homology searches were conducted using the *Sv*FeCH protein sequence as a query against the NCBI non-redundant protein as described above, virtually all the top hits were bacterial sequences excluding the sequences of filarial nematodes (data not shown). These findings prompted us to conduct a phylogenetic analysis to better clarify the evolutionary origin of nematode FeCH genes.

Phylogenetic Analysis

The amino acid alignment of FeCH sampled from 71 eukaryotic and 71 bacterial species was phylogenetically analyzed by ML and Bayesian methods (Figure 3). Overall, the FeCH trees inferred by the ML and Bayesian methods were concordant with each other as well as the results of previously published FeCH phylogenies [7,46,47,48]. Four major clades including the FeCH homologues sampled from eukaryotes were reconstructed with ML bootstrap support values (MLBPs) of 86%–96% and a Bayesian posterior probability (BPP) of 1.00 (shaded in blue, green, pink, and orange; Figure 3): (1) a 'blue' clade comprising a single bacterial homolog (*Gemmatimonas aurantiaca*) and those of eukaryotes–non-nematode metazoans, fungi, *Capsaspora owczarzaki*, oomycetes, amoebozoans, and ciliates; (2) a 'green' clade of the homolog of cyanobacteria including an obligate endosymbiont in the testate amoeba, *Paulinella chromatophora* [49], and putative plastid homolog in photosynthetic eukaryotes; (3) a 'pink' clade comprising the homolog of insect trypanosomatids [3]; (4) an 'orange' clade comprising the homolog of parasitic nematodes including *S. venezuelensis*. Other homologs sampled from eukaryotes were scattered amongst the bacterial homologues, and they exhibited no specific evolutionary affinity to other homologs.

The FeCH phylogeny suggested that the homologs from non-nematode metazoans nested in the 'blue' clade and those of nematodes forming the 'orange' clade were distantly related to each other. Although they received little support from the ML bootstrap and Bayesian analyses, the homologs from non-nematode metazoans, *Capsaspora*, and fungi were grouped together, corresponding to members of Opisthokonta, a well-established monophyletic assemblage [50]. Curiously, the nematode FeCH homologs formed a robust clade with an MLBP of 96% and BPP of 1.00, being distinct from other metazoan homologs. This tree topology can be rationalized by the vertical inheritance of FeCH genes from the ancestral opisthokont species to non-nematode metazoans and horizontal transfer of a FeCH gene between the ancestral nematodes and a non-metazoan organism. This conjecture was further supported by a topology test comparing the ML tree shown in Figure 3 with three alternative trees, in which the nematode homologs were enforced to branch at the base of (1) the non-nematode metazoan clade, (2) the clade of the opisthokont homologues (excluding that of *Schizosaccharomyces pombe*), and (3) the 'blue' clade composed of the eukaryotic and *Gemmatimonas* homologs (highlighted by diamonds in Figure 3). Importantly, all the alternative trees were successfully rejected with very small p values (2.0×10^{-78}–2.0×10^{-36}).

Chelatase Assay using Recombinant *Sv*FeCH

To determine whether the FeCH gene of *S. venezuelensis* identified in the present study encodes an active enzyme, we conducted a chelatase assay using a bacterially expressed recombinant *Sv*FeCH. We constructed an expression plasmid, pET-*Sv*FeCH, which was used to transform *E. coli* strain BL21. Protein expression was induced by incubation with 0.3 mM IPTG at 30°C for 2 h. The enzyme activity was measured using the cell extracts of untransformed and transformed bacteria. The FeCH activity in transformed bacteria, which was derived from over-expressed *Sv*FeCH and endogenous *E. Coli* FeCH, was much higher than that in the untransformed control, which originated solely from endogenous FeCH, indicating that the enzyme was active (Figure. 4).

Genetic Complementation Assay of hemH Deficient *E. coli*

The VS200 strain of *E. coli* K12, a hemH null-mutant, was used for the gene complementation assay, and the results are shown in Figure 5. VS200 could not grow in LB medium, unless hemin (10 μg/ml) was supplemented. The expression of *Sv*FeCH by pFLAG-CTC-*Sv*FeCH made the bacteria capable of growing in the LB medium in the absence of hemin. Transforming the bacteria with the control vector (pFLAG-CTC) did not have such an effect. Therefore, it was concluded that *Sv*FeCH is an active enzyme that can function as FeCH.

Expression of FeCH during the Life Cycle of *S. venezuelensis*

The relative expression levels of *Sv*FeCH mRNA were assessed by real-time RT-PCR analysis using RNA samples prepared from the six major developmental stages of *S. venezuelensis* (Figure 6). It was observed that although *Sv*FeCH mRNA expression was present throughout the stages, it was relatively low in L3i.

Discussion

We demonstrated that a gene for FeCH exists in the *S. venezuelensis* genome. Although the presence of the FeCH gene in the draft genome of *B. malayi* was reported previously [24,25], no further characterization was reported. The present study represents the first cloning and characterization of nematode FeCH, particularly in an evolutionary context.

Phylogenetic analyses revealed that nematode FeCH forms a distinct clade from that of non-nematode metazoans, indicating that the evolutionary origin of nematode FeCH is fundamentally different from that of the FeCH genes of other metazoan organisms. In the ML phylogeny, the nematode clade was placed within the homologs from a subset of alpha-proteobacteria, although the statistical support for this hypothesis is inconclusive. If the affinity between the nematode and alpha-proteobacterial FeCH homologs is genuine, then an as-yet-unknown alpha-proteobacterium was the source of the FeCH homologs working in the extant nematodes. This hypothesis is intriguing because replacement of the eukaryotic FeCH gene by a bacterial FeCH gene had been suggested only for unicellular eukaryotes, such as apicomplexan parasites (*Plasmodium falciparum, P. chabaudi, P. berghei, Eimeria tenella, Toxoplasma gondii,* and *Neospora caninum*) [47,48,51], the chromerid *Chromera velia* [47], rhodophytes (*Cyanidioschyzon merolae, Porphyra yezoensis,* and *Galdieria sulphuraria*) [48], and the euglenid *Euglena gracilis* [46].

BLAST analysis of the sequenced nematode genomes and transcriptomes revealed that the FeCH gene is present only in *Strongyloides* (clade IV) and filarial parasites (clade III). It is still not clear at which point of nematode evolution the proposed horizontal gene transfer event occurred. Regarding *B. malayi* and related filarial nematodes, horizontal gene transfer from *Wolbachia*, a bacterial symbiont, is known to have occurred [52]. However, the FeCH sequences present in nematode genomes do not appear to originate from *Wolbachia* based on the positions of the *Wolbachia* species in the phylogenetic tree (Figure 3).

We hypothesize two possible scenarios concerning the evolutionary histories of FeCH genes in nematodes, using a current view of the phylogenetic relationship of nematode clades [10]. Because no nematode species possesses the 'blue clade' FeCH commonly found in opisthokonts, it can be speculated that this type of FeCH was lost early in nematode evolution (Figure. 7). *Strongyloides* and the filarias may have acquired FeCH genes from alpha-proteobacteria independently. Alternatively, a common ancestral lineage leading to clades III, IV, and V may have received such an alpha-proteobacterial FeCH gene (scenarios 1 and 2, respectively: Fig. 7a and 7b). For scenario 1 to be true, the hypothetical alpha-proteobacterial species that provided FeCH genes to *Strongyloides* and filarias, need to be closely related to each other, because the nematode homologs were robustly grouped together in the FeCH phylogeny (Figure. 3). In scenario 2, the lateral transfer of a bacterial FeCH gene occurred through an ancestor leading to species that belong to clades III, IV, and V, and again, the FeCH gene disappeared in some species in clades III and IV such as *Ascaris* and *Meloidogyne* and in the branch leading to clade V (Figure. 7b).

Among the parasitic nematodes, the reason why only *Strongyloides* and filarias needed to reacquire (scenario 1) or retain (scenario 2) FeCH gene is unclear, particularly when the other six heme biosynthesis genes are still absent. This situation (the presence of FeCH gene in the absence of other heme biosynthesis genes) has been documented for a limited number of organisms, such as *Haemophilus influenzae* [53] and *P. serpens* [9]. As was suggested for *H. influenzae* [9,54], there may be a possibility that FeCH is used to obtain Fe^{2+} through its reverse activity rather than obtain heme from protoporphyrin IX using its forward activity.

Supporting Information

Table S1 List of primers used in this study.
(PDF)

Table S2 Taxonomic affiliation and accession numbers for the sequences considered in the phylogenetic analysis.
(PDF)

Table S3 BLAST homology search against predicted proteins from nematode genome projects.
(PDF)

Table S4 BLAST homology search against nematode EST database (NEMBASE 4).
(PDF)

Table S5 BLAST homology search against nematode EST database (NEMBASE 4) using *Strongyloides venezuelensis* ferrochelatase sequence as a query.
(PDF)

Table S6 Sequence similarities of FeCH proteins assessed by BLAST program.
(PDF)

Acknowledgments

SI is a research fellow supported by the Japan Society for Promotion of Sciences for Young Scientists (No. 00007). We thank Dr. Tadasuke Ooka (University of Miyazaki, Japan) for helpful discussions and Amy Hombu (University of Miyazaki) for critical reading of the manuscript.

Author Contributions

Conceived and designed the experiments: EN HM. Performed the experiments: EN ST GC AY. Analyzed the data: SI YI. Wrote the paper: EN SI YI HM.

References

1. Furuyama K, Kaneko K, Vagras P (1997) Heme as a magnificent molecule with multiple missions: Heme determines its own fate and governs cellular homeostasis. Tohoku J Exp Med 213: 1–116.
2. Dailey HA (1997) Enzymes of heme biosynthesis. JBIC 2: 411–417.
3. Koreny L, Lukes J, Obornik M (2010) Evolution of the haem synthetic pathway in kinetoplastid flagellates: an essential pathway that is not essential after all? Int J Parasitol 40: 149–156.
4. Chang KP, Chang CS, Sassa S (1975) Heme biosynthesis in bacterium-protozoon symbioses: enzymic defects in host hemoflagellates and complemental role of their intracellular symbiotes. Proc Natl Acad Sci U S A 72: 2979–2983.
5. Berriman M, Ghedin E, Hertz-Fowler C, Blandin G, Renauld H, et al. (2005) The genome of the African trypanosome *Trypanosoma brucei*. Science 309: 416–422.
6. El-Sayed NM, Myler PJ, Bartholomeu DC, Nilsson D, Aggarwal G, et al. (2005) The genome sequence of *Trypanosoma cruzi*, etiologic agent of Chagas disease. Science 309: 409–415.
7. Alves JM, Voegtly L, Matveyev AV, Lara AM, da Silva FM, et al. (2011) Identification and phylogenetic analysis of heme synthesis genes in trypanosomatids and their bacterial endosymbionts. PLoS One 6: e23518.
8. Chang KP, Trager W (1974) Nutritional significance of symbiotic bacteria in two species of hemoflagellates. Science 183: 531–532.
9. Koreny L, Sobotka R, Kovarova J, Gnipova A, Flegontov P, et al. (2012) Aerobic kinetoplastid flagellate *Phytomonas* does not require heme for viability. Proc Natl Acad Sci U S A 109: 3808–3813.
10. Sommer RJ, Streit A (2011) Comparative genetics and genomics of nematodes: genome structure, development, and lifestyle. Annu Rev Genet 45: 1–20.
11. Blaxter ML, De Ley P, Garey JR, Liu LX, Scheldeman P, et al. (1998) A molecular evolutionary framework for the phylum Nematoda. Nature 392: 71–75.
12. The C. elegans Sequencing Consortium (1998) Genome sequence of the nematode *C. elegans*: a platform for investigating biology. Science 282: 2012–2018.
13. Rao AU, Carta LK, Lesuisse E, Hamza I (2005) Lack of heme synthesis in a free-living eukaryote. Proc Natl Acad Sci U S A 102: 4270–4275.
14. Blaxter ML (1993) Nemoglobins: divergent nematode globins. Parasitol Today 9: 353–360.
15. Minning DM, Gow AJ, Bonaventura J, Braun R, Dewhirst M, et al. (1999) Ascaris haemoglobin is a nitric oxide-activated 'deoxygenase'. Nature 401: 497–502.
16. Takamiya S, Hashimoto M, Kazuno S, Kikkawa M, Yamakura F (2009) *Ascaris suum* NADH-methemo(myo)globin reductase systems recovering differential functions of hemoglobin and myoglobin, adapting to environmental hypoxia. Parasitol Int 58: 278–284.
17. Amino H, Osanai A, Miyadera H, Shinjyo N, Tomitsuka E, et al. (2003) Isolation and characterization of the stage-specific cytochrome b small subunit (CybS) of *Ascaris suum* complex II from the aerobic respiratory chain of larval mitochondria. Mol Biochem Parasitol 128: 175–186.
18. Viney ME, Lok JB (2007) *Strongyloides* spp. WormBook: 1–15.
19. Bethony J, Brooker S, Albonico M, Geiger SM, Loukas A, et al. (2006) Soil-transmitted helminth infections: ascariasis, trichuriasis, and hookworm. The Lancet 367: 1521–1532.
20. Montes M, Sawhney C, Barros N (2010) *Strongyloides stercoralis*: there but not seen. Curr Opin Infect Dis 23: 500–504.
21. Sato Y, Toma H (1990) *Strongyloides venezuelensis* infections in mice. Int J Parasitol 20: 57–62.
22. Nagayasu E, Ogura Y, Itoh T, Yoshida A, Chakraborty G, et al. (2013) Transcriptomic analysis of four developmental stages of *Strongyloides venezuelensis*. Parasitol Int 62: 57–65.
23. Ferreira GC (1999) Ferrochelatase. Int J Biochem Cell Biol 31: 995–1000.
24. Wu B, Novelli J, Foster J, Vaisvila R, Conway L, et al. (2009) The heme biosynthetic pathway of the obligate *Wolbachia* endosymbiont of *Brugia malayi* as a potential anti-filarial drug target. PLoS Negl Trop Dis 3: e475.
25. Ghedin E, Wang S, Spiro D, Caler E, Zhao Q, et al. (2007) Draft genome of the filarial nematode parasite *Brugia malayi*. Science 317: 1756–1760.
26. Maruyama H, El-Malky M, Kumagai T, Ohta N (2003) Secreted adhesion molecules of *Strongyloides venezuelensis* are produced by oesophageal glands and are components of the wall of tunnels constructed by adult worms in the host intestinal mucosa. Parasitology 126: 165–171.

27. Scotto-Lavino E, Du G, Frohman MA (2006) 3′ end cDNA amplification using classic RACE. Nat Protoc 1: 2742–2745.
28. Scotto-Lavino E, Du G, Frohman MA (2006) 5′ end cDNA amplification using classic RACE. Nat Protoc 1: 2555–2562.
29. Altschul SF, Gish W, Miller W, Myers EW, Lipman DJ (1990) Basic local alignment search tool. J Mol Biol 215: 403–410.
30. Stein LD, Bao Z, Blasiar D, Blumenthal T, Brent MR, et al. (2003) The genome sequence of *Caenorhabditis briggsae*: a platform for comparative genomics. PLoS Biol 1: E45.
31. Dieterich C, Clifton SW, Schuster LN, Chinwalla A, Delehaunty K, et al. (2008) The *Pristionchus pacificus* genome provides a unique perspective on nematode lifestyle and parasitism. Nat Genet 40: 1193–1198.
32. Opperman CH, Bird DM, Williamson VM, Rokhsar DS, Burke M, et al. (2008) Sequence and genetic map of Meloidogyne hapla: A compact nematode genome for plant parasitism. Proc Natl Acad Sci U S A 105: 14802–14807.
33. Kikuchi T, Cotton JA, Dalzell JJ, Hasegawa K, Kanzaki N, et al. (2011) Genomic insights into the origin of parasitism in the emerging plant pathogen *Bursaphelenchus xylophilus*. PLoS Pathog 7: e1002219.
34. Jex AR, Liu S, Li B, Young ND, Hall RS, et al. (2011) *Ascaris suum* draft genome. Nature 479: 529–533.
35. Mitreva M, Jasmer DP, Zarlenga DS, Wang Z, Abubucker S, et al. (2011) The draft genome of the parasitic nematode *Trichinella spiralis*. Nat Genet 43: 228–235.
36. Elsworth B, Wasmuth J, Blaxter M (2011) NEMBASE4: the nematode transcriptome resource. Int J Parasitol 41: 881–894.
37. Margulies M, Egholm M, Altman WE, Attiya S, Bader JS, et al. (2005) Genome sequencing in microfabricated high-density picolitre reactors. Nature 437: 376–380.
38. Katoh K, Kuma K, Toh H, Miyata T (2005) MAFFT version 5: improvement in accuracy of multiple sequence alignment. Nucleic Acids Res 33: 511–518.
39. Stamatakis A, Hoover P, Rougemont J (2008) A rapid bootstrap algorithm for the RAxML Web servers. Syst Biol 57: 758–771.
40. Tanabe AS (2011) Kakusan4 and Aminosan: two programs for comparing nonpartitioned, proportional and separate models for combined molecular phylogenetic analyses of multilocus sequence data. Mol Ecol Resour 11: 914–921.
41. Ronquist F, Teslenko M, van der Mark P, Ayres DL, Darling A, et al. (2012) MrBayes 3.2: efficient Bayesian phylogenetic inference and model choice across a large model space. Syst Biol 61: 539–542.
42. Taketani S, Ishigaki M, Mizutani A, Uebayashi M, Numata M, et al. (2007) Heme synthase (ferrochelatase) catalyzes the removal of iron from heme and demetalation of metalloporphyrins. Biochemistry 46: 15054–15061.
43. Nakahigashi K, Nishimura K, Miyamoto K, Inokuchi H (1991) Photosensitivity of a protoporphyrin-accumulating, light-sensitive mutant (visA) of *Escherichia coli* K-12. Proc Natl Acad Sci U S A 88: 10520–10524.
44. Kohno H, Okuda M, Furukawa T, Tokunaga R, Taketani S (1994) Site-directed mutagenesis of human ferrochelatase: identification of histidine-263 as a binding site for metal ions. Biochim Biophys Acta 1209: 95–100.
45. Dailey HA, Dailey TA, Wu CK, Medlock AE, Wang KF, et al. (2000) Ferrochelatase at the millennium: structures, mechanisms and [2Fe-2S] clusters. Cell Mol Life Sci 57: 1909–1926.
46. Koreny L, Obornik M (2011) Sequence evidence for the presence of two tetrapyrrole pathways in *Euglena gracilis*. Genome Biol Evol 3: 359–364.
47. Koreny L, Sobotka R, Janouskovec J, Keeling PJ, Obornik M (2011) Tetrapyrrole synthesis of photosynthetic chromerids is likely homologous to the unusual pathway of apicomplexan parasites. Plant Cell 23: 3454–3462.
48. Obornik M, Green BR (2005) Mosaic origin of the heme biosynthesis pathway in photosynthetic eukaryotes. Mol Biol Evol 22: 2343–2353.
49. Nakayama T, Ishida K (2009) Another acquisition of a primary photosynthetic organelle is underway in *Paulinella chromatophora*. Curr Biol 19: R284–285.
50. Wainright PO, Hinkle G, Sogin ML, Stickel SK (1993) Monophyletic origins of the metazoa: an evolutionary link with fungi. Science 260: 340–342.
51. Sato S, Wilson RJ (2003) Proteobacteria-like ferrochelatase in the malaria parasite. Curr Genet 42: 292–300.
52. Dunning Hotopp JC, Clark ME, Oliveira DC, Foster JM, Fischer P, et al. (2007) Widespread lateral gene transfer from intracellular bacteria to multicellular eukaryotes. Science 317: 1753–1756.
53. Schlor S, Herbert M, Rodenburg M, Blass J, Reidl J (2000) Characterization of ferrochelatase (hemH) mutations in *Haemophilus influenzae*. Infect Immun 68: 3007–3009.
54. Loeb MR (1995) Ferrochelatase activity and protoporphyrin IX utilization in *Haemophilus influenzae*. J Bacteriol 177: 3613–3615.
55. Larkin MA, Blackshields G, Brown NP, Chenna R, McGettigan PA, et al. (2007) Clustal W and Clustal X version 2.0. Bioinformatics 23: 2947–2948.
56. Medlock AE, Dailey TA, Ross TA, Dailey HA, Lanzilotta WN (2007) A pi-helix switch selective for porphyrin deprotonation and product release in human ferrochelatase. J Mol Biol 373: 1006–1016.

Parasitology International 62 (2013) 57–65

Contents lists available at SciVerse ScienceDirect

Parasitology International

journal homepage: www.elsevier.com/locate/parint

Transcriptomic analysis of four developmental stages of *Strongyloides venezuelensis*

Eiji Nagayasu [a], Yoshitoshi Ogura [b], Takehiko Itoh [c], Ayako Yoshida [a], Gunimala Chakraborty [a], Tetsuya Hayashi [b], Haruhiko Maruyama [a,*]

[a] Department of Infectious Diseases, Division of Parasitology, Faculty of Medicine, University of Miyazaki, 5200 Kihara Kiyotake, Miyazaki 889-1692, Japan
[b] Division of Bioenvironmental Science, Frontier Science Research Center, University of Miyazaki, 5200 Kihara, Kiyotake, Miyazaki 889-1692, Japan
[c] Department of Biological Information, Graduate School of Bioscience and Biotechnology, Tokyo Institute of Technology, 4259 Nagatsuta-cho, Midori-ku, Yokohama 226-8501, Japan

ARTICLE INFO

Article history:
Received 19 April 2012
Received in revised form 2 September 2012
Accepted 20 September 2012
Available online 27 September 2012

Keywords:
Strongyloides
Animal-parasitic nematode
Transcriptome

ABSTRACT

Strongyloides venezuelensis is one of some 50 species of genus *Strongyloides*, obligate gastrointestinal parasites of vertebrates, responsible for strongyloidiasis in humans and other domestic/companion animals. Although *S. venezuelensis* has been widely used as a model species for studying human/animal strongyloidiasis, the sequence information for this species has been quite limited. To create a more comprehensive catalogue of expressed genes for identification of genes potentially involved in animal parasitism, we conducted a de novo sequencing analysis of the transcriptomes from four developmental stages of *S. venezuelensis*, using a Roche 454 GS FLX Titanium pyrosequencing platform. A total of 14,573 contigs were produced after de novo assemblies of over 2 million sequencing reads and formed a dataset "Vene454". BLAST homology search of Vene454 against proteome and transcriptome data from other animal-parasitic and non-animal-parasitic nematode species revealed several interesting genes, which may be potentially related to animal parasitism, including nicotinamide phosphoribosyltransferase and ferrochelatase. The Vene454 dataset analysis also enabled us to identify transcripts that are specifically enriched in each developmental stage. This work represents the first large-scale transcriptome analysis of *S. venezuelensis* and the first study to examine the transcriptome of the lung L3 developmental stage of any *Strongyloides* species. The results not only will serve as valuable resources for future functional genomics analyses to understand the molecular aspects of animal parasitism, but also will provide essential information for ongoing whole genome sequencing efforts in this species.

1. Introduction

Members of the genus *Strongyloides* are gastrointestinal parasites of vertebrates, some of which are pathogens of medical and veterinary importance. The life cycle of *Strongyloides* is rather complex but fascinating from a biological perspective [1]. Infective 3rd stage larvae (L3i) live in soil and infect the host animal by penetrating the skin. The larvae migrate through the connective tissue, enter the circulation, and then reach the lung. They escape into the alveolar space, ascend the tracheobronchial tree, get swallowed, and finally reach the small intestine, where they molt twice into parasitic adults. Eggs produced by the adult worms hatch into first stage larvae (L1) in the host intestine or in the host feces depending on the species. These larvae either develop directly into L3i through 2 molts (direct development) or into free-living worms of either sex (indirect development). In case of the indirect development, adult worms of male and female mate to produce eggs in the soil. The L1 progeny of this generation develops into L3i in most species. However, more than one free-living cycle are known to occur in some species [2].

More than 52 *Strongyloides* species are recognized so far. Among them, two species are known to cause human diseases (strongyloidiasis), affecting an estimated 50–100 million individuals worldwide [3]. Of the 2 species, *Strongyloides stercoralis* is much more widespread than the other species, *S. fuelleborni* [4]. Several species infect livestock, including *S. ransomi* in swine [5], *S. westeri* in horses [6] and *S. papillosus* in ruminants [7]. Companion animals (dogs and cats) are also affected by some *Strongyloides* species, such as *S. stercoralis* and *S. planiceps* [4,8].

For laboratory studies, *Strongyloides ratti* and *Strongyloides venezuelensis* are the most widely used [9]. Both the species are native to rats but can also infect mice. Large scale EST analysis of *Strongyloides* parasites was first conducted for *S. ratti* using L1, L2, free-living adult/L3i, and parasitic females [10]. A total of 4152 clusters were obtained from this analysis which were estimated to be the 20% of the *S. ratti* genes and later used for developing a microarray assay system [11,12]. Large scale EST analysis was also conducted for *S. stercoralis*, which generated 3311 EST clusters, using L1- and L3i-stage libraries [13]. More recently, a transcriptome analysis of *S. stercoralis* L3i using 454/Roche pyrosequencing technology [14] was also reported [15]. However for *S.*

* Corresponding author at: 5200 Kihara, Kiyotake, Miyazaki 889-1692, Japan. Tel.: +81 985 85 0990; fax: +81 985 84 3887.
E-mail address: hikomaru@med.miyazaki-u.ac.jp (H. Maruyama).

1383-5769/$ – see front matter © 2012 Elsevier Ireland Ltd. All rights reserved.
http://dx.doi.org/10.1016/j.parint.2012.09.006

venezuelensis, only limited EST data (162 clusters from an L3i library) have been reported so far [16].

In this study, our aim was to create a more comprehensive catalogue of expressed genes for *S. venezuelensis*, which enables us to perform comparative analyses with the rapidly expanding transcriptome data from other free-living and parasitic nematodes.

Using the 454/Roche pyrosequencing technology, we analyzed non-normalized cDNA libraries constructed from four developmental stages, including lung third-stage larvae (LL3) which were not studied in the previous *S. ratti* and *S. stercoralis* EST analyses. The LL3 stage is present in a wide variety of animal-parasitic nematodes belonging to different phylogenetic clades, such as *Ascaris* and *Toxocara* in clade III, *Necator* and *Nippostrongylus* in clade V and *Strongyloides* in clade IV. However, the biological significance of this stage is not well understood [17]. In *S. venezuelensis*, both L3i and LL3 are in the third stage, but they show considerable biological differences. For example, L3i can penetrate the host's skin but they are unable to do so at the LL3 stage [17]. Moreover, L3i cannot settle down in the intestinal mucosa but LL3 can, secreting adhesion molecules [17,18]. Therefore a major developmental change seems to take place during the transition from L3i to LL3.

At present, our understanding on many aspects of biology of *Strongyloides* parasites at the molecular level is quite limited, so the large-scale transcriptome analysis carried out in this study will help in prioritizing and accelerating researches in this understudied genus.

2. Materials and methods

2.1. Parasites and animals

S. venezuelensis used in this study was originally isolated at Naha, Okinawa, Japan by Hasegawa and others in 1988 [19]. Since then, this isolate has been maintained by serial passages in laboratory rats: feces from infected rats were cultured using the filter paper method [20] for 3–4 days and infective third stage larvae (L3i) which came out of the feces were collected. These larvae were used to infect next rats. Because one infection cycle typically takes 10 days, it was estimated that this *S. venezuelensis* isolate had been maintained for roughly 800 generations before the sample collection (done in 2010) for this study. At the time of the original isolation, it was already noticed that this strain of *S. venezuelensis* produced very few numbers of free-living stages [19]. In our hands, no free-living stage has been observed so far. Therefore, it appears that the ability to undertake free-living development has been lost for this strain of *S. venezuelensis* during the long laboratory maintenance. For this reason, free-living stages were not included in the present study.

ICR mice and Wistar rats were purchased from Kyudo Co. Ltd. (Kumamoto, Japan). All animals were kept and handled under the approval of the Animal Experiment Committee of the University of Miyazaki. The third-stage infective larvae (L3i) were obtained from fecal culture by the filter paper method [21]. For collection of the lung third-stage larvae (LL3), male ICR mice were subcutaneously inoculated with approximately 30,000 L3i, and the lungs were removed 72–75 h post infection (p.i.), homogenized with Polytron PT-MR3000 (Kinematica AG, Littau, Switzerland) at 20,000 rpm for a few seconds. The lung homogenates were wrapped with KimWipe papers and incubated in phosphate-buffered saline (PBS) at 37 °C for 1.5 h and worms emerging out through the paper were collected [22]. Mixtures of eggs and first stage larvae (L1) were collected as follows: eggs were separated from feces by the flotation method with saturated salt solution [23], washed extensively with water, and incubated at 27 °C for 24 h in PBS. About half of the eggs hatched into L1. This egg/L1 mixture was collected by centrifugation. Parasitic adult female worms were collected from infected rats 8–10 days p.i. [22].

2.2. Preparation of transcriptome libraries and 454 sequencing

Frozen worms were crushed manually using a freeze-crushing apparatus (SK Mill, Tokken, Chiba, Japan), followed by total RNA isolation with the TRIzol reagent (Invitrogen, Carlsbad, CA, USA) [16].

Four cDNA libraries from each of the 4 different developmental stages (Egg/L1, L3i, LL3, and adults) were prepared for 454 sequencing according to the manufacturer's instruction [24], with each library having different MID (Titanium Multiplex Identifier) adaptors. Two sequencing runs were performed with the Roche 454 GS FLX Titanium platform to generate 543,713 reads, 622,248 reads, 679,257 reads and 638,728 reads for Egg/L1, L3i, LL3 and adult stages, respectively.

2.3. Assembly of 454 reads

Pooled sequencing reads from the four stages were subjected to assembling by the Roche's de novo GS assembler (Newbler, release 2.3). The initial 14,892 contig sequences were first searched against the NCBI nucleotide database (nt) and the NCBI Rat UniGene sequences using the BLASTn program. Contigs which showed BLAST hits to bacterial, viral or *Rattus norvegicus* nucleotide sequences and ribosomal RNA sequences ($<1e^{-40}$) were removed from the dataset. The remaining 14,573 contigs formed a dataset "Vene454" and were subjected for further analyses.

2.4. Functional gene classification based on gene ontology and protein family/domain search

Functional annotation by the gene ontology (GO) terms was carried out using the Blast2GO (B2G) program [25]. InterPro (InterProScan, EBI) search was performed remotely from B2G via the InterPro EBI webserver [26,27].

2.5. BLAST homology search

Sequences in the Vene454 dataset were subjected to BLAST [28] analysis against predicted protein data from the following nematode genome projects: *Caenorhabditis briggsae* (nematode clade V) [29], *Caenorhabditis elegans* (V) [30], *Caenorhabditis japonica* (V) [31], *C. remanei* (V) [31], *Caenorhabditis brenneri* (V) [31], *Meloidogyne incognita* (IV) [32], *Meloidogyne hapla* (IV) [33], *Bursaphelenchus xylophilus* (IV) [34], *Brugia malayi* (III) [35], *Ascaris suum* (III) [36], and *Trichinella spiralis* (I) [37]. BLAST analyses were also performed against nematode ESTs (expressed sequence tags) from NEMBASE4 [38]. In this case, from the original NEMBASE4, which contains 237,154 EST clusters from 62 nematode species, 2 sub-datasets were generated. One was composed of 114,356 clusters from 33 animal-parasitic species and the other contained 101,450 from 25 non-animal-parasitic (i.e. free-living or plant parasitic) species. Species included in each sub-dataset are listed in Table S1.

Contig sequences showed BLAST hits (BLAST score cut-off = 50) to protein or EST sequences of multiple animal-parasitic species that belong to multiple clades in the absence of BLAST hits (BLAST score cut-off = 40) to the following free-living and plant parasitic nematode species: *C. elegans*, *C. briggsae*, *C. brenneri*, *C. japonica*, *M. hapla*, *M. incognita*, and *B. xylophilus* (protein sequences), and species listed as non-animal-parasitic in Table S1 (EST sequences), were considered to be potential animal parasitism related genes. Among such *S. venezuelensis* contigs, only those with sequence descriptions by the Blast2GO program were selected. The original sequence descriptions generated by the Blast2GO program were sometimes uninformative, so we manually curated them when necessary.

2.6. Expression pattern profiling during development

Expression pattern profiling of each gene was conducted with CLC genomics workbench 5.1 (CLC bio, Aarhus, Denmark). In this analysis,

sequences in the Vene454 dataset were used as references, and sequencing reads originating from each stage were mapped to the references. The numbers of reads which were uniquely mapped to each contig (read counts) were considered as measures for the expression level of each gene. A transcript (contig) was designated to be stage-enriched when the read count belonged to the top 15% in abundance in one stage whereas the read counts for the same gene were ≤3 in all other stages.

3. Results

3.1. Pyrosequencing and de novo assembly

We obtained 2,483,165 sequencing reads from 2 sequencing runs, in which the average read length was 389 nucleotides (nt). The sequencing data have been deposited to DDBJ Sequence Read Archive (DRA) under the accession number DRA000395. These sequencing reads were assembled into 14,902 contigs using NEWBLER v.2.3. This initial dataset was subjected to BLASTn search to remove the rRNA sequences and the sequences of bacterial, viral or host animal (rat) origin. The remaining 14,573 sequences formed a dataset "Vene454".

3.2. Functional gene classification based on gene ontology and by InterPro domain/family search

Gene ontology (GO) terms for the three main categories (cellular component, biological process and molecular functions) were assigned to sequences in the Vene454 dataset using the Blast2GO program. A total of 66,204 GO terms were mapped to 9574 out of the 14,573 contigs queried (an average of 4.5 GO terms/contigs). To have a general overview of the assigned terms, Blast2GO scores [39] calculated for each GO terms (level 2) in the three main categories are summarized in Table S2.

Sequence search against the InterPro database was also conducted to extrapolate potential functions based on the sequence signatures of the predicted proteins. A summary of the 20 most frequent domains and families found in the Vene454 dataset is shown in Table S3. The most frequently identified protein family was IPR00276 (7 transmembrane G-protein coupled receptor, rhodopsin-like), which forms an extraordinary large gene family in *C. elegans* as well that plays key roles in chemoreception [40]. It was also noticeable that there were 140 contigs that were predicted to have IPR001506 (Peptidase M12A, astacin).

3.3. BLAST similarity search and identification of potential animal-parasitism-related genes

We tried to find out contigs of which potential homologues could not be found in any of the non-animal parasites while potential homologues were found in animal parasites beyond clade IV to which *S. venezuelensis* belongs. A total of 2218 contigs showed that BLAST hits to sequences in at least one animal-parasitic species, while no hit was found in any of free-living and plant-parasitic species. Among them, only 55 contigs had sequence descriptions assigned by the Blast2GO program. From these 55 contigs, 18 were removed because potential homologous sequences seemed to exist only in the clade IV animal parasites. At this point manual curations of the automatically assigned descriptions were conducted and resulted in a removal of 25 sequences because of their uninformative descriptions. A list of the 12 remaining sequences is presented in Table 1. This list includes several genes of interesting functions such as nicotinamide phosphoribosyltransferase (contig04650), an enzyme involved in the processing of nicotinamide adenine dinucleotide (NAD) in mammals, deoxyribodipyrimidine photolyase (contig08989), a light-driven DNA repair enzyme, tuberin (contig10542) an intracellular signaling molecule, and a ferrochelatase gene (contig10320) which produces an enzyme in the heme biosynthetic pathway. Four contigs (contigs12792, 13180, 13181 and 14229) encode proteins with SCP (sperm coating protein) domains, which are implicated in various host–pathogen interactions in parasitic helminthes [41].

3.4. Expression pattern profiling

Strongyloides experience an entirely different environments during development. Their adaptation to the environment should be

Table 1
Potential animal parasitism genes identified by BLAST homology searches against animal-parasitic and non-animal-parasitic nematode sequences. *S. venezuelensis* contigs that showed BLAST hits to protein or EST sequences from multiple animal-parasitic species which belong to multiple clades in the absence of BLAST hits to the following free-living and plant-parasitic nematode species; *Caenorhabditis elegans, Caenorhabditis briggsae, Caenorhabditis brenneri, Caenorhabditis japonica, Meloidogyne hapla, Meloidogyne incognita, Bursaphelenchus xylophilus*, and species listed as non-animal-parasitic species in Table S1, were considered to be potential animal parasitism related gene and presented in this table. Sequence descriptions were retrieved automatically (unmarked) or assigned manually (marked with asterisk). When the presence of signal peptides (SP) or transmembrane domains (TM) was predicted by the Blast2GO program, they are shown in the table. Abbreviated species names are presented when respective contig sequence showed BLAST hit to sequences in proteome database (in red color) or EST database (in black color): Ts (*Trichinella spiralis*), Tm (*Trichuris muris*), As (*Ascaris suum*), Bm (*Brugia malayi*), Ls (*Litomosoides sigmodontis*), Ov (*Onchocerca volvulus*) Ss (*Strongyloides stercoralis*), Sv (*Strongyloides venezuelensis*) Sr (*Strongyloides ratti*), Dv (*Dictyocaulus viviparus*), Pt (*Parastrongyloides trichosuri*) Ac (*Ancylostoma caninum*), Hc (*Haemonchus contortus*), and Oo (*Ostertagia ostertagi*).

				Potential orthologue in animal parasitic nematodes			
				Clade			
Sequence ID	Length	Description	Signal peptide (SP), transmembrane domain (TM)	I	III	IV	V
Contig04650	1514	Nicotinamide phosphoribosyltransferase		Ts, Ts, Tm	As, Bm	Sv	Ac
Contig08989	891	Deoxyribodipyrimidine photo-lyase-like		Ts	As, Bm	Sv	
Contig10542	1042	Tuberin isoform 4		Ts	As, Bm	Sv	
Contig12682	1239	Putative myelin proteolipid protein*	SP, TM		As, Bm	Sv, Sr, Dv	Ac
Contig01173	1116	Ubiquitin-associated domain-containing protein*	SP, TM		As, Bm, As	Sv, Ss, Sr	
Contig03678	794	Nuclear hormone receptor-like 1			As, Bm	Sv	
Contig03812	526	Hypothetical protein*			As, Bm	Sv	
Contig03855	1748	Gamma-tubulin complex component, putative			As	Sv	
Contig10320	934	Ferrochelatase			Bm, Ls, Ov	Sv, Sr	
Contig12792	732	Golgi-associated plant pathogenesis related protein (GAPR)-like*	SP			Sv, Sr, Ss, Pt	Ac
Contig13180	806	Golgi-associated plant pathogenesis related protein (GAPR)-like*	SP			Sv, Sr, Ss, Pt	Ac
Contig13181	736	Golgi-associated plant pathogenesis related protein (GAPR)-like*	SP			Sv, Sr, Ss, Pt	Ac
Contig14229	694	Golgi-associated plant pathogenesis related protein (GAPR)-like*	SP			Sv, Sr, Ss, Pt	Ac

Table 2
Transcripts enriched at each developmental stage. Sequence reads originated from the each developmental stage were mapped to contig sequences. The number of reads which were uniquely mapped to each contig, was considered as measures for the expression level. See Materials and methods for the inclusion criteria. Sequence descriptions were obtained automatically by Blast2GO program (unmarked) or manually (marked with asterisk). When BLAST hits were found by species specific database search (cut-off BLAST score > 50), the identifiers of the top-hit sequences were presented. Mean, median and range of the BLAST scores for hits presented in the four tables are as follows: Clade IV; 212, 152 (51–1456), Clade III; 213, 156 (51–1174), and Clade V; 223, 116 (52–1168).

NA: no description available.

Sequence ID	Length (nt)	Description	Number of reads				BLAST top hit sequence ID					
							Clade IV			Clade III		Clade V
			Egg_L1	L3i	Lung	Adults	*S. ratti*	*S. stercoralis*	*M. incognita*	*B. malayi*	*A. suum*	*C. elegans*
(a) Egg/1st stage larvae												
Contig02224	6321	C-type lectin-like domain containing protein*	320	2	0	0	SRC00288	SSC05703	–	BM02362	GS_11180	F40F4.6
Contig00944	1807	Acid sphingomyelinase*	179	2	1	0	SRC03337	–	WBMinc15253	–	GS_00745	ZK455.4
Contig13529	2623	—NA—	98	0	2	2	SRC01061	–	–	–	–	-
Contig02791	1117	Phospholipase membrane-associated-like	66	2	2	3	SRC00315	SSC03181	WBMinc04650	BM01697	GS_14039	F09C8.1
Contig09089	953	Collagen family member*	62	0	0	0	SRC00419	SSC02818	WBMinc01401b	BM18921	GS_12613	C29F4.1
Contig05231	1563	Hypothetical protein*	60	0	2	1	SRC02227	–	–	–	–	C12D12.1c
Contig06547	1023	Cuticle collagen	34	60	0	0	0	SRC00651	SSC02603	WBMinc01401a	BM18921	GS_15592
Contig13207	666	—NA—	51	1	0	0	SRC07045	SSC02645	–	–	–	–
Contig11888	780	Hypothetical protein*	45	0	0	0	WBMinc09904	BM20167	GS_08342	C42D4.3		
Contig04606	984	Collagen family member (col-107)	44	0	0	1	SRC01306	SSC02645	WBMinc06657	BM06181	GS_11454	K08C9.4
Contig08342	882	Cre-grl-4 protein (hedgehog-like protein)*	44	0	0	0	SRC00831	SSC01751	WBMinc08602	BM21849	GS_00656	F42C5.7
Contig03141	2120	Cre-glnA-2 protein (putative glutaminase)*	42	1	0	1	SRC02034	SSC06043	WBMinc05738	BM06061	GS_03196	DH11.1
Contig13485	1149	Hypothetical protein*	41	0	1	1	SRC02258	SSC02457	–	–	–	–
Contig03829	1765	Cre-Tyr-2 protein (tyrosinase family member)*	38	0	0	0	SRC01066	SSC03597	WBMinc17501	BM00502	GS_03401	K08E3.1
Contig14061	1067	—NA—	38	0	1	0	–	–	–	–	–	–
Contig13553	838	—NA—	37	0	2	0	–	–	–	–	–	–
Contig07887	2658	Laminin subunit alpha-1-like	32	0	1	1	SRC02207	–	WBMinc07462	BM06796	GS_04625	T22A3.8
Contig10636	2031	TBC (Tre-2/Bub2/Cdc16) domain family member*	32	1	1	0	SRC00690	SSC03889	WBMinc17739c		GS_04011	C31E10.8
Contig07078	3565	Cell adhesion molecule	31	2	3	2	–	–	WBMinc00828	BM19509	GS_11487	Y54G2A.25a
Contig01949	914	—NA—	30	0	0	0	SRC00448	–	–	–	–	-
Contig02995	1002	Acid ceramidase-like	30	0	0	0	SRC02798	–	–	BM04865	GS_09726	F27E5.1
Contig08108	618	—NA—	30	2	1	0	–	–	–	–	–	–
Contig09136	893	C-type lectin family member*	29	0	3	2	SRC00609	–	WBMinc16602	BM21558	GS_03260	F08H9.9
Contig06835	832	Hypothetical protein	25	1	1	2	–	SSC00728	–	–	GS_18776	D1053.3
Contig04087	1854	Nuclear hormone receptor family member*	23	1	3	1	SRC05235	SSC03578	WBMinc15420	BM00476	GS_17444	K08A2.5a
Contig11995	1385	Sybindin-like family protein	23	1	0	0	SRC02156	SSC02451	WBMinc15567	BM06401	GS_22622	K04H4.2a
Contig13448	1185	Collagen family member*	23	0	2	0	SRC09545	SSC02645	WBMinc17140	BM19392	GS_10172	B0222.8
Contig14273	1033	Histidine ammonia-lyase	23	0	2	2	–	–	WBMinc18775	–	GS_22677	F47B10.2
Contig01037	1292	Frizzled smoothened family membrane region containing protein	20	0	2	2	–	–	WBMinc15075	BM20979	GS_09630	Y71F9B.5b
Contig03437	2088	Pan domain-containing protein	20	0	0	3	SRC00996	SSC02945	WBMinc04213a	BM01345	GS_19262	C34G6.6a
(b) Infective 3rd stage larvae												
Contig02069	1411	Zinc metalloproteinase nas-34	0	1717	0	0	SRC00539	SSC00003	WBMinc08611	BM21202	GS_18837	F40E10.1
Contig08387	923	Zinc metalloproteinase nas-34*	0	1522	3	0	SRC00539	SSC00003	WBMinc08611	BM21202	GS_18837	F40E10.1
Contig04750	1054	Hypothetical protein*	0	1203	0	0	–	–	–	–	–	–
Contig08029	602	—NA—	0	772	0	0	–	–	–	–	–	–
Contig11278	698	Zinc metalloproteinase nas-8	1	674	0	0	SRC04332	SSC00003	WBMinc18862	BM01052	GS_04549	C24F3.3
Contig08808	874	Zinc metalloproteinase nas-37*	0	401	0	0	SRC00539	SSC00003	WBMinc08611	BM21202	GS_18850	C17G1.6b
Contig10138	1492	L3NieAg.01 [*Strongyloides stercoralis*]*	0	336	0	0	SRC08538	SSC00683	WBMinc17117a	BM01273	GS_17544	F09B9.5
Contig11702	833	Zinc metalloproteinase nas-34	0	278	0	0	SRC00539	SSC00003	WBMinc08611	BM07170	GS_18837	F40E10.1
Contig12649	1931	Zinc metalloproteinase nas-10*	1	153	2	0	SRC05342	SSC00042	WBMinc12125	BM03357	GS_22487	K09C8.3a
Contig14343	1290	Golgi-associated plant pathogenesis-related protein 1	0	146	0	0	SRC08538	SSC00135	WBMinc18383	BM06834	GS_17544	C07A4.3
Contig13830	1092	—NA—	0	135	0	0	–	–	–	–	–	–
Contig14054	648	Golgi-associated plant pathogenesis-related protein 1	0	99	0	0	SRC08538	SSC00135	–	BM05783	GS_17544	D2062.1
Contig07246	544	L3NieAg.01 [*Strongyloides stercoralis*]	0	87	0	0	SRC08538	SSC00443	–	–	–	–

Contig12331	760	Zinc metalloproteinase nas-34	0	76	0	0	SRC00539	SSC00003	WBMinc08611	BM07170	GS_18837	F40E10.1
Contig10178	735	—NA—	0	71	0	0	–	–	–	–	–	–
Contig13298	736	—NA—	0	66	0	0	–	–	–	–	–	–
Contig12705	1305	Zinc metalloproteinase nas-34*	0	50	1	0	SRC00539	SSC00042	WBMinc08611	BM02087	GS_19601	F40E10.1
Contig07767	781	—NA—	0	48	3	0	–	–	–	–	–	–
Contig13315	1118	Zinc metalloproteinase nas-35*	0	47	2	0	–	–	WBMinc08611	BM02087	GS_22432	R151.5b
Contig03997	1072	Ethanolamine kinase 2	2	46	3	0	–	–	WBMinc08582	BM19004	GS_11400	T27A10.3a
Contig13646	1566	Beta-carotene 15,15′-monooxygenase family member*	2	46	1	1	–	–	–	–	GS_06216	F53C3.12
Contig00684	1170	Oxidoreductase dhs-27	2	42	1	0	SRC00538	–	WBMinc11865	–	GS_05517	C04F6.5
Contig03297	1078	Zinc metalloproteinase nas-34*	0	41	2	0	–	–	–	BM02521	GS_19601	F40E10.1
Contig08423	2233	Fatty acid CoA synthetase family member*	1	40	3	0	SRC00384	SSC02675	WBMinc17074	BM00321	GS_21585	C46F4.2
Contig06231	1258	—NA—	2	38	0	0	SRC00328	SSC05998	–	–	–	–
Contig13434	559	—NA—	0	38	0	0	–	–	–	–	–	–
Contig10214	1952	Cytochrome p450 3a31	2	37	0	1	SRC03666	–	WBMinc02462	BM18491	GS_07692	T10B9.10
Contig13065	843	—NA—	0	35	0	0	SRC00328	SSC05998	–	–	–	–
Contig04331	956	Nematode cuticle collagen n-terminal domain containing protein	0	34	0	0	SRC03961	SSC02645	WBMinc17140	BM19392	GS_10172	F54D1.3
(c) Lung 3rd stage larvae												
Contig03540	670	—NA—	0	1	216	2	–	–	–	–	–	-
Contig13070	655	—NA—	0	0	143	3	–	–	–	–	–	–
Contig13069	661	—NA—	0	0	125	1	–	–	–	–	–	–
Contig09901	1346	Zinc metalloproteinase nas-34*	0	0	123	0	SRC00539	SSC00003	WBMinc08611	BM02087	GS_07714	F40E10.1
Contig13633	1019	OSM-11 protein	0	0	79	0	–	–	–	–	–	F11C7.5
Contig10229	1087	Zinc metalloproteinase nas-34*	0	0	75	2	–	–	WBMinc08611	BM03110	GS_18837	F40E10.1
Contig06113	528	Transthyretin-like protein*	2	1	56	1	SRC01301	SSC02724	WBMinc14072	BM20212	GS_02516	T07C12.7
Contig02851	1086	Venom allergen-like 11 protein	0	0	52	0	–	–	–	–	–	–
Contig10105	920	Golgi-associated plant pathogenesis related protein (GAPR)-like*	0	0	52	1	SRC08538	SSC00599	WBMinc16018	BM01805	GS_17544	C07A4.3
Contig11886	961	Estradiol 17-beta-dehydrogenase 12-like	0	0	47	0	SRC05398	–	WBMinc04612	BM20233	GS_19420	F56D1.5
Contig12786	1308	Zinc metalloproteinase nas-34	0	0	45	0	SRC03714	SSC00042	WBMinc08611	BM02087	GS_18850	R151.5b
Contig12598	782	OSM-11 protein*	0	1	44	0	–	–	–	–	–	F11C7.5
Contig06348	1088	—NA—	0	0	43	0	–	–	–	–	–	–
Contig07825	879	Zinc metalloproteinase nas-35*	0	0	40	0	SRC03714	SSC00042	WBMinc01936	BM21202	GS_18850	R151.5b
Contig12613	535	Golgi-associated plant pathogenesis related protein (GAPR)-like*	0	0	38	0	–	SSC00683	–	–	–	–
Contig06196	684	Methylmalonyl epimerase	0	1	37	1	–	SSC02207	–	–	GS_04860	D2030.5
Contig11090	2368	Ionotropic glutamate receptor*	3	2	37	2	–	–	WBMinc16875	BM04228	GS_04745	C43H6.9
Contig13975	1157	Hypothetical protein*	0	1	37	0	–	–	–	–	–	–
Contig00485	1132	Golgi-associated plant pathogenesis related protein (GAPR)-like*	2	0	35	2	SRC04034	–	–	–	GS_03132	T05A10.5
Contig09819	815	Zinc metalloproteinase nas-34*	0	0	35	0	SRC00539	SSC00042	WBMinc08611	BM02087	GS_07714	F40E10.1
Contig09049	1059	Nudix (nucleoside diphosphate linked some moiety X) hydrolase*	3	3	34	1	–	SSC01175	WBMinc04889	–	–	T26E3.2
Contig11769	905	Hypothetical protein*	1	0	32	0	–	–	–	–	GS_22053	Y53G8AM.5
Contig14038	798	Methylmalonyl epimerase	0	0	32	2	–	SSC02207	–	–	GS_04860	D2030.5
Contig03008	1369	Gelsolin*	1	0	31	3	SRC05220	–	WBMinc01119	BM18400	GS_06329	K06A4.3
Contig07091	644	Ribosomal protein l10ae	0	0	31	0	SRC00046	SSC02482	WBMinc05373	BM04544	GS_02386	Y71F9AL.13a
Contig10797	970	—NA—	3	0	31	1	SRC02185	–	–	–	GS_22490	–
Contig12871	1298	Zinc metalloproteinase nas-34*	0	0	30	0	SRC06107	SSC00042	WBMinc08611	BM21202	GS_19601	F40E10.1
Contig00194	818	Phosphomannomutase	2	0	29	3	SRC05571	–	WBMinc02970	BM19329	GS_01521	F52B11.2
Contig04923	1991	Alpha-mannosidase 2	0	0	29	0	–	–	WBMinc02404	BM06489	GS_16932	F58H1.1b
Contig12080	1006	TWiK family of potassium channels family member*	0	1	29	0	SRC00944	–	WBMinc12795	BM21499	GS_12849	F31D4.7
(d) Parasitic adults												
Contig10124	955	—NA—	0	0	1	2512	–	–	–	–	–	–
Contig14181	516	—NA—	0	0	0	2078	–	–	–	–	–	–
Contig10244	1883	Low-density lipoprotein receptor domain class a containing protein	0	0	1	2053	SRC00284	–	WBMinc19129	BM19101	GS_19807	B0244.8
Contig13969	714	—NA—	0	0	0	1825	–	–	–	–	–	–
Contig08064	877	—NA—	0	0	1	1654	–	–	–	–	–	–
Contig13154	576	—NA—	1	0	0	1562	–	–	–	–	–	–
Contig07567	578	—NA—	0	0	1	1332	–	–	–	–	–	–
Contig13491	678	—NA—	0	0	1	1180	–	–	–	–	–	–
Contig06493	1416	K homology RNA-binding domain containing protein*	0	0	0	860	SRC02447	SSC03190	WBMinc12667	BM18433	GS_19572	T21G5.5c

(continued on next page)

Table 2 (*continued*)

Sequence ID	Length (nt)	Description	Number of reads				BLAST top hit sequence ID					
							Clade IV			Clade III		Clade V
			Egg_L1	L3i	Lung	Adults	*S. ratti*	*S. stercoralis*	*M. incognita*	*B. malayi*	*A. suum*	*C. elegans*
Contig05703	1092	Hypothetical protein*	1	0	1	821	SRC06045	–	–	–	–	–
Contig06367	1541	Neprilysin metallopeptidase*	0	0	0	773	SRC05161	–	WBMinc16791	BM20231	GS_17345	ZK20.6
Contig00162	700	Small heat shock protein	1	0	2	739	SRC03310	SSC05811	WBMinc03043	BM11415	GS_06997	F52E1.7b
Contig06375	650	—NA—	0	0	2	671	–	–	–	–	–	–
Contig12735	2941	Chitin binding peritrophin-a domain protein	3	0	0	605	SRC03421	–	WBMinc04227	BM17021	GS_06014	C39D10.7
Contig07950	1939	Low-density lipoprotein receptor domain class a containing protein	2	0	1	575	SRC00284	–	WBMinc19129	BM19101	GS_19807	B0244.8
Contig08916	2847	Leucine rich repeat family protein	0	0	0	475	SRC04599	–	WBMinc12978	BM19603	GS_02665	K07A12.2
Contig06477	584	—NA—	0	0	0	449	–	–	–	–	–	–
Contig10027	1144	—NA—	0	0	1	413	SRC03394	–	–	–	–	–
Contig10496	1775	Protein-tyrosine phosphatase containing protein	0	0	3	404	SRC02931	–	WBMinc10481	BM18273	GS_18620	F44F4.2
Contig02443	1830	Chitin binding peritrophin-a domain protein	2	0	2	364	SRC03826	–	WBMinc04227	BM02152	GS_23600	H02I12.1
Contig00263	4536	Chitin binding peritrophin-a domain protein	0	0	0	361	SRC03421	–	WBMinc04227	BM17021	GS_06014	C39D10.7
Contig00269	4534	Chondroitin proteoglycan*	0	0	0	297	SRC03421	–	WBMinc04227	BM17021	GS_06014	C39D10.7
Contig02852	861	—NA—	0	0	0	232	SRC05206	–		BM05768		C44B12.1
Contig13778	536	Chondroitin proteoglycan*	1	0	0	224	SRC01117	–	WBMinc00448		GS_04563	F52E1.5
Contig08830	713	—NA—	0	0	1	222	SRC03581	–	–	–	–	–
Contig05882	1232	Zinc metalloproteinase nas-34*	0	0	0	198	–	–	WBMinc08611	BM02521	–	F40E10.1
Contig10183	2033	—NA—	0	0	0	184	SRC03497	–	–	–	–	–
Contig06424	1623	Protein kinase*	0	0	0	183	SRC03455	–	WBMinc07137	BM18075	GS_10043	F19H6.1
Contig03795	738	—NA—	0	0	0	172	SRC01128	–	–	–	–	–
Contig00094	2507	Recq-mediated genome instability protein 1-like	0	0	0	170	–	–	–	BM21827	GS_20775	M01E11.3
Contig06589	1037	—NA—	1	0	0	168	SRC04208	–	–	–	–	–
Contig07090	2820	Patched family protein	1	0	1	165	SRC06840	–	WBMinc00357	BM05698	GS_05730	C32E8.8
Contig03718	1346	Hypothetical protein*	2	0	0	160	–	WBMinc04027b	Y39G10AR.18a			
Contig00354	760	—NA—	2	0	0	151	SRC03196	–	–	–	–	–
Contig02385	2162	Methylmalonyl-CoA mutase, mitochondrial*	1	0	2	146	SRC05460	SSC03218	–	–	GS_20654	ZK1058.1
Contig01101	804	—NA—	0	0	0	139	–	–	–	–	–	–
Contig09645	843	—NA—	0	0	0	139	–	–	–	–	–	–
Contig01871	1826	Septin*	0	0	0	136	SRC03332	–	WBMinc03825	BM16658	GS_01629	Y50E8A.4b
Contig10147	1759	—NA—	0	0	0	132	SRC03497	–	–	–	–	–
Contig07387	4672	Chitin synthase	0	0	0	129	SRC02107	–	WBMinc05474	BM02779	GS_05696	T25G3.2
Contig10224	1124	—NA—	0	0	0	127	–	–	–	–	–	–
Contig06580	738	—NA—	0	0	0	125	SRC01128	–	–	–	–	–
Contig00014	929	lysozyme*	1	0	0	123	SRC01535	SSC03202	WBMinc18568	BM01191	GS_22190	C17G10.5
Contig06202	2875	Chitin binding peritrophin-a domain protein	3	0	0	122	SRC05734	–	WBMinc04514	BM02152	GS_06014	R02F2.4
Contig10746	1191	Nanos RNA binding domain containing protein	1	0	1	119	SRC04796	–	WBMinc07136	BM20002		R03D7.7
Contig01639	1031	—NA—	1	0	0	105	SRC05193	–	–	–	–	–
Contig06752	2062	Peroxidase*	0	0	0	104	SRC00904	SSC05870	WBMinc14864	BM06085	GS_10747	F49E12.1
Contig06374	758	e3 ubiquitin-protein ligase march2	0	0	0	103	SRC05118	–	WBMinc07559	BM20137	GS_12562	C17E4.3
Contig10067	2721	Ankyrin repeat protein	3	0	3	100	–	–	WBMinc14479	BM19330	GS_21230	T28D6.4
Contig03411	2880	Hypothetical protein*	3	0	1	92	SRC08065	–	–	BM01867	–	–

reflected in the corresponding expression profiles of larvae and adult worms. In order to identify transcripts that are enriched at a specific developmental stage, number of reads which were uniquely mapped to each contig was used as an indicator of expression abundance. The distribution of read counts for the 14,573 is shown in Fig. S1. When a read count for a given contig is among the highest 15% (>17 counts at Egg/L1, >11 at L3i, >25 at LL3 and >24 at parasitic adults) at one particular stage, but less than or equal to 3 at other stages, that contig was considered as being enriched at this particular stage. There were 33, 68, 37 and 226 such contigs enriched at Egg/L1, L3i, LL3 and parasitic adults, respectively. Among these contigs top 30 (Egg/L1, L3i, LL3) and 50 (parasitic adults) sequences in abundance at each stage were selected and presented in Table 2.

In the Egg/L1 stage, a number of genes in this list were annotated as a structural component of worm body or cells, such as collagens (contigs09080, 06547, 04606, and 13448), tyrosinase (contig03829), cross-linking of cuticular collagens [42] and laminin (contig07887), a component of the basement membrane [43].

In the L3i stage being ready for infection, there were nine stage-enriched transcripts (contigs02069, 08387, 11278, 08808, 11702, 12649, 12705, 13315, and 03297), which were identified as nematode astacin-like zinc metalloproteases (NAS). Two contigs (contigs10138 and 07246) were identified as homologues of L3Nie antigen of *S. stercoralis*, an important immunodiagnostic antigen for this species [44].

In the LL3 stage, there were 6 genes (contigs09901, 10229, 12786, 07825, 09819 and 12871) also identified as nematode astacin-like zinc metalloproteases. Other genes of interests include OSM-11 (contig12598); a co-activator for Notch receptor, implicated in defecation and osmotic resistance in *C. elegans* [45]. Two genes (contigs00194; phosphomannomutase, and 04923; alpha-mannosidase) involved in the glycan biosynthetic reactions were noticeable.

In the parasitic adult stage, among 50 selected contigs, no sequence description could be assigned to 21 (42%) contigs (shown as "NA"). In all of these cases, BLAST hits could not be found in any of the species in clade III, IV or V shown in the table, except 8 contigs to which potential *S. ratti* homologues could be found (contigs10027, 08830, 10183, 03795, 06589, 00354, 10147, and 01639). Most enriched transcripts included contigs10244 and 07950 that showed homology to a *C. elegans* gene for Egg-1 (B2044.8), an oocyte plasma membrane protein, most likely reflecting active oogenesis at this stage. Four genes (contigs12735, 02443, 00263, and 06202) coded chitin binding peritrophin-a domain protein, which is thought to be involved in eggshell formation in *C. elegans* [46].

4. Discussion

Here we describe the first large-scale transcriptomic analysis of four developmental stages in *S. venezuelensis*, one of the model species to study human/animal strongyloidiasis and biology of animal-parasitic nematodes. The 454 pyrosequencing technology used in the present study greatly expanded the database of sequence information on this species. Furthermore, a number of the stage-enriched transcripts were identified. Such transcripts potentially hold keys to understand molecular mechanisms of various aspects of the parasite biology, such as host-skin invasion, tissue migration, settlement in the mucosa of the small intestine, and immune evasion.

One astonishing finding in the present study was that *S. venezuelensis* appears to possess many different astacin-like zinc metalloproteases. Astacin-like zinc metalloprotease genes form a large gene family in *C. elegans* (39 intact- and 1 pseudogenes), and they play a variety of roles in digestion, hatching, peptide processing, morphogenesis and pattern formation of nematodes [47]. In parasitic nematodes, astacin-like zinc metalloproteases have been implicated in skin invasion ability [48–54]. The results of our analysis indicate that the astacin-like zinc metalloprotease gene family of *S. venezuelensis* might be even larger. We found 182 contigs that showed top BLAST hits to one of the 39 *C. elegans* astacin-like zinc metalloprotease genes (Table S4). Among the 182 contigs, 130 were confirmed to possess the astacin peptidase domain (IPR001506). Interestingly, a different set of astacin-like metalloprotease genes appeared to be up-regulated when L3i and LL3 were compared (Table 2). This may explain the differences in invasion and migration abilities between L3i and LL3. This is also interesting from the evolutionary point of view. Future analysis of the phylogenetic relationship of *Strongyloides* and *C. elegans* astacin-like zinc metalloprotease family genes may provide insights into how parasitic phenotypes such as skin invasion and tissue migration abilities had been evolved.

BLAST analyses using transcriptomic data obtained in this study identified three enzyme genes, which were found to be shared by multiple animal-parasitic species beyond the phylogenetic clades, but have not be found in any of the free-living or plant-parasitic species. One was nicotinamide phosphoribosyltransferase (NAMPT), the rate-limiting enzyme in the salvage pathway of NAD biosynthesis from nicotinamide. Considering NAMPT has been believed to be an enzyme of vertebrates [55,56], it is quite interesting to find NAMPT genes in diverse members of nematode parasites of vertebrates. Intriguingly, this enzyme was also reported to act as a cytokine (pre-B-cell colony enhancing factor 1 (PBEF-1)) that promotes B cell maturation and inhibits neutrophil apoptosis [57]. It will be interesting to analyze why animal-parasitic nematodes including *S. venezuelensis* need this protein, especially in relation to the interaction with the host immune system.

Another enzyme which appears only in animal-parasitic nematodes is ferrochelatase. It catalyzes the last step of the heme biosynthetic pathway, which is an insertion of ferrous iron into protoporphyrin IX to form the heme. It was reported that *C. elegans* lacks all seven enzymes required to synthesize heme from the first universal precursor, δ-aminolevulinic acid. We could not find other enzymes for this pathway in Vene454 dataset (data not shown). This situation (presence of only the ferrochelatase gene among the genes for heme biosynthetic pathway) is reminiscent of the cases in *B. malayi* (animal-parasitic nematode) and in trypanosomatid protozoa [58]. Because studies on a mammalian ferrochelatase demonstrated that it can also catalyze a reverse reaction (removal of iron from heme) other than the well-studied forward reaction (insertion of iron into protoporphyrin IX) [59], this enzyme in *S. venezuelensis* may be required for the acquisition of iron which is not readily available in the animal host [60].

The third enzyme which appears only in animal-parasitic nematodes is deoxyribodipyrimidine photolyase, an enzyme which is involved in repair of DNA legions caused by UV radiation [61]. Exposure to the sunlight can occur to some animal parasites (*Ascaris suum* (eggs), and *Strongyloides* (eggs and larval stages)) which were found to possess the gene for this enzyme. However, *T. spiralis*, and *B. malayi* also have this enzyme gene and do not have a developmental stage which is directly exposed to the sunlight. Therefore the biological significance of possessing this enzyme remains to be investigated.

We included the migrating larval stage in the lung (LL3) in this transcriptomic analysis, which was not examined in the previous large-scale transcriptomic sequencing efforts in other *Strongyloides* species [10,13]. Although this stage exists in some animal parasitic nematodes beyond phylogenetic clades, including *Strongyloides* (clade IV), *Ascaris* (clade III) and *Necator* (clade V), its biological significance is still unclear. Because no large-scale transcriptomic analysis of LL3 stage has been reported for any of these species to our knowledge, the present study serves as an important addition to the existing nematode transcriptome databases.

Once the larvae reach the lung, they need to escape from the blood vessel into the alveolar space. This process requires the breakage of blood vessels and the alveolar tissues in the lung. Multiple astacin-like metalloprotease transcripts were identified to be specifically enriched in LL3. These proteases may be involved in this process causing

proteolytic tissue degradation. We found potential *osm-11* homologues which showed stage-enriched expressions in LL3. Studies in *C. elegans* show that OSM-11 is a secreted, diffusible protein, which acts as a ligand for Notch receptor (LIN-12)-mediated signaling pathway [45]. Other than osmotic resistance [62], multiple roles were reported for OSM-11, including the vulval development [45]. In *C. elegans* it was reported that the vulval development spans from L3 to late L4. Divisions of primary vulval precursor cells occur by the late L3 [63,64]. Therefore it is possible that the lung-stage L3 is initiating vulval development under the influence of OSM-11, even though the structure is not grossly visible at that stage.

We identified two LL3 stage-enriched expressions of genes that encode enzymes involved in glycan biosynthetic reactions (phosphomannomutase, alpha-mannosidase). Parasitic helminthes including nematodes release numerous types of proteins into the host environment as part of E/S (excretory/secretory) products [65]. These parasite E/S products are generally rich in glycoproteins [66], leading to many potential interactions with innate pattern recognition receptors including Toll-like receptors and C-type lectins on host dendritic cells [66]. The enriched expression of the glycan biosynthetic genes might be a reflection of elevated production of such glycoproteins.

5. Conclusion

Our study generated lists of *S. venezuelensis* genes that are potentially important in animal parasitism based on the phylogenetic distribution and the stage-enriched expression. Although computational assembly and annotation should be carefully verified experimentally, this study has provided a first glimpse of the transcriptome of *S. venezuelensis*, and very valuable information for prioritizing future research areas with a number of interesting genes discussed above. The data obtained in this study will serve as resources for different types of high-throughput studies, such as DNA microarray and proteome analyses.

Supplementary data to this article can be found online at http://dx.doi.org/10.1016/j.parint.2012.09.006.

Acknowledgments

This work was supported by grants from the Ministry of Education, Culture, Sports, Science and Technology of Japan (Grant-in-Aid for Scientific Research C 21590466, Grant-in-Aid for Young Scientists B 23790461, and Grant-in-Aid for Scientific Research on Priority Areas 'Matrix of Infection Phenomena' 21022041), the Ministry of Health, Labor and Welfare (H23-Shinko-Ippan-014, H23-Kokui-Shitei-003, and H22-Seisakusouyaku-Ippan-003), and the University of Miyazaki (Integrated Research Project for Human and Animal Medicine).

We also acknowledge the kind support and assistance from the Support Programs for Genome Science (Genome-Shien), established by the Ministry of Education, Culture, Sports, Science and Technology of Japan.

References

[1] Viney ME, Lok JB. Strongyloides spp. WormBook 2007:1–15.
[2] Yamada M, Matsuda S, Nakazawa M, Arizono N. Species-specific differences in heterogonic development of serially transferred free-living generations of *Strongyloides planiceps* and *Strongyloides stercoralis*. Journal of Parasitology 1991;77:592-4.
[3] Carvalho EM, Da Fonseca Porto A. Epidemiological and clinical interaction between HTLV-1 and *Strongyloides stercoralis*. Parasite Immunology 2004;26:487-97.
[4] Speare R. Identification of species of *Strongyloides*. London/New York/Philadelphia: Taylor & Francis; 1989.
[5] Stewart TB, Stone WM, Marti OG. *Strongyloides ransomi*: prenatal and transmammary infection of pigs of sequential litters from dams experimentally exposed as weanlings. American Journal of Veterinary Research 1976;37:541-4.
[6] Netherwood T, Wood JL, Townsend HG, Mumford JA, Chanter N. Foal diarrhoea between 1991 and 1994 in the United Kingdom associated with *Clostridium perfringens*, rotavirus, *Strongyloides westeri* and *Cryptosporidium* spp. Epidemiology and Infection 1996;117:375-83.
[7] Eberhardt AG, Mayer WE, Bonfoh B, Streit A. The *Strongyloides* (Nematoda) of sheep and the predominant *Strongyloides* of cattle form at least two different, genetically isolated populations. Veterinary Parasitology 2008;157:89-99.
[8] Itoh N, Muraoka N, Aoki M, Itagaki T. Prevalence of Strongyloides spp. infection in household dogs. Kansenshōgaku Zasshi 2003;77:430-5.
[9] Sato Y, Toma H. *Strongyloides venezuelensis* infections in mice. International Journal for Parasitology 1990;20:57-62.
[10] Thompson FJ, Mitreva M, Barker GL, Martin J, Waterston RH, McCarter JP, et al. An expressed sequence tag analysis of the life-cycle of the parasitic nematode *Strongyloides ratti*. Molecular and Biochemical Parasitology 2005;142:32-46.
[11] Thompson FJ, Barker GL, Hughes L, Wilkes CP, Coghill J, Viney ME. A microarray analysis of gene expression in the free-living stages of the parasitic nematode *Strongyloides ratti*. BMC Genomics 2006;7:157.
[12] Thompson FJ, Barker GL, Hughes L, Viney ME. Genes important in the parasitic life of the nematode *Strongyloides ratti*. Molecular and Biochemical Parasitology 2008;158:112-9.
[13] Mitreva M, McCarter JP, Martin J, Dante M, Wylie T, Chiapelli B, et al. Comparative genomics of gene expression in the parasitic and free-living nematodes *Strongyloides stercoralis* and *Caenorhabditis elegans*. Genome Research 2004;14:209-20.
[14] Margulies M, Egholm M, Altman WE, Attiya S, Bader JS, Bemben LA, et al. Genome sequencing in microfabricated high-density picolitre reactors. Nature 2005;437:376-80.
[15] Marcilla A, Garg G, Bernal D, Ranganathan S, Forment J, Ortiz J, et al. The transcriptome analysis of *Strongyloides stercoralis* L3i larvae reveals targets for intervention in a neglected disease. PLoS Neglected Tropical Diseases 2012;6:e1513.
[16] Yoshida A, Nagayasu E, Nishimaki A, Sawaguchi A, Yanagawa S, Maruyama H. Transcripts analysis of infective larvae of an intestinal nematode, *Strongyloides venezuelensis*. Parasitology International 2011;60:75-83.
[17] Maruyama H, Nishimaki A, Takuma Y, Kurimoto M, Suzuki T, Sakatoku Y, et al. Successive changes in tissue migration capacity of developing larvae of an intestinal nematode, *Strongyloides venezuelensis*. Parasitology 2006;132:411-8.
[18] Maruyama H, El-Malky M, Kumagai T, Ohta N. Secreted adhesion molecules of *Strongyloides venezuelensis* are produced by oesophageal glands and are components of the wall of tunnels constructed by adult worms in the host intestinal mucosa. Parasitology 2003;126:165-71.
[19] Hasegawa H, Orido Y, Sato Y, Otsuru M. *Strongyloides venezuelensis* Brumpt, 1934 (Nematoda: Strongyloididae) collected from *Rattus norvegicus* in Naha, Okinama, Japan. Japanese Journal of Parasitology 1988;37:429-34.
[20] Islam MK, Matsuda K, Kim JH, Baek BK. Effects of in vitro culture methods on morphological development and infectivity of *Strongyloides venezuelensis* filariform larvae. The Korean Journal of Parasitology 1999;37:13-9.
[21] Korenaga M, Nawa Y, Mimori T, Tada I. *Strongyloides ratti*: the role of enteral antigenic stimuli by adult worms in the generation of protective immunity in rats. Experimental Parasitology 1983;55:358-63.
[22] Maruyama H, Yabu Y, Yoshida A, Nawa Y, Ohta N. A role of mast cell glycosaminoglycans for the immunological expulsion of intestinal nematode, *Strongyloides venezuelensis*. Journal of Immunology 2000;164:3749-54.
[23] Baek BK, Islam MK, Kim JH. Development of an in vitro culture method for harvesting the free-living infective larvae of *Strongyloides venezuelensis*. The Korean Journal of Parasitology 1998;36:15-22.
[24] Roche Diagnostics. cDNA rapid library preparation method manualGS FLX titanium series; 2009.
[25] Conesa A, Gotz S, Garcia-Gomez JM, Terol J, Talon M, Robles M. Blast2GO: a universal tool for annotation, visualization and analysis in functional genomics research. Bioinformatics 2005;21:3674-6.
[26] Hunter S, Apweiler R, Attwood TK, Bairoch A, Bateman A, Binns D, et al. InterPro: the integrative protein signature database. Nucleic Acids Research 2009;37:D211-5.
[27] Quevillon E, Silventoinen V, Pillai S, Harte N, Mulder N, Apweiler R, et al. InterProScan: protein domains identifier. Nucleic Acids Research 2005;33:W116-20.
[28] Altschul SF, Gish W, Miller W, Myers EW, Lipman DJ. Basic local alignment search tool. Journal of Molecular Biology 1990;215:403-10.
[29] Stein LD, Bao Z, Blasiar D, Blumenthal T, Brent MR, Chen N, et al. The genome sequence of *Caenorhabditis briggsae*: a platform for comparative genomics. PLoS Biology 2003;1:E45.
[30] The *C. elegans* sequencing consortium. Genome sequence of the nematode *C. elegans*: a platform for investigating biology. Science 1998;282:2012-8.
[31] Stein L, Sternberg P, Durbin R, Thierry-Mieg J, Spieth J. WormBase: network access to the genome and biology of *Caenorhabditis elegans*. Nucleic Acids Research 2001;29:82-6.
[32] Abad P, Gouzy J, Aury JM, Castagnone-Sereno P, Danchin EG, Deleury E, et al. Genome sequence of the metazoan plant-parasitic nematode *Meloidogyne incognita*. Nature Biotechnology 2008;26:909-15.
[33] Opperman CH, Bird DM, Williamson VM, Rokhsar DS, Burke M, Cohn J, et al. Sequence and genetic map of *Meloidogyne hapla*: a compact nematode genome for plant parasitism. Proceedings of the National Academy of Sciences of the United States of America 2008;105:14802-7.
[34] Kikuchi T, Cotton JA, Dalzell JJ, Hasegawa K, Kanzaki N, McVeigh P, et al. Genomic insights into the origin of parasitism in the emerging plant pathogen *Bursaphelenchus xylophilus*. PLoS Pathogens 2011;7:e1002219.
[35] Ghedin E, Wang S, Spiro D, Caler E, Zhao Q, Crabtree J, et al. Draft genome of the filarial nematode parasite *Brugia malayi*. Science 2007;317:1756-60.
[36] Jex AR, Liu S, Li B, Young ND, Hall RS, Li Y, et al. *Ascaris suum* draft genome. Nature 2011;479:529-33.
[37] Mitreva M, Jasmer DP, Zarlenga DS, Wang Z, Abubucker S, Martin J, et al. The draft genome of the parasitic nematode *Trichinella spiralis*. Nature Genetics 2011;43:228-35.
[38] Elsworth B, Wasmuth J, Blaxter M. NEMBASE4: the nematode transcriptome resource. International Journal for Parasitology 2011;41:881-94.

[39] Gotz S, Garcia-Gomez JM, Terol J, Williams TD, Nagaraj SH, Nueda MJ, et al. High-throughput functional annotation and data mining with the Blast2GO suite. Nucleic Acids Research 2008;36:3420-35.
[40] Robertson HM, Thomas JH. The putative chemoreceptor families of *C. elegans*. WormBook 2006:1–12.
[41] Cantacessi C, Hofmann A, Young ND, Broder U, Hall RS, Loukas A, et al. Insights into SCP/TAPS proteins of liver flukes based on large-scale bioinformatic analyses of sequence datasets. PLoS One 2012;7:e31164.
[42] Gerrits D, Blaxter M. Tyrosinases of *Caenorhabditis elegans*. International *C. elegans* meeting; 1995.
[43] Huang CC, Hall DH, Hedgecock EM, Kao G, Karantza V, Vogel BE, et al. Laminin alpha subunits and their role in *C. elegans* development. Development 2003;130:3343-58.
[44] Ravi V, Ramachandran S, Thompson RW, Andersen JF, Neva FA. Characterization of a recombinant immunodiagnostic antigen (NIE) from *Strongyloides stercoralis* L3-stage larvae. Molecular and Biochemical Parasitology 2002;125:73-81.
[45] Komatsu H, Chao MY, Larkins-Ford J, Corkins ME, Somers GA, Tucey T, et al. OSM-11 facilitates LIN-12 Notch signaling during *Caenorhabditis elegans* vulval development. PLoS Biology 2008;6:e196.
[46] Johnston WL, Krizus A, Dennis JW. Eggshell chitin and chitin-interacting proteins prevent polyspermy in *C. elegans*. Current Biology 2010;20:1932-7.
[47] Park JO, Pan J, Mohrlen F, Schupp MO, Johnsen R. Baillie DL, et al. Characterization of the astacin family of metalloproteases in C elegans BMC Developmental Biology 2010;10:14.
[48] Borchert N, Becker-Pauly C, Wagner A, Fischer P, Stocker W, Brattig NW. Identification and characterization of onchoastacin, an astacin-like metalloproteinase from the filaria *Onchocerca volvulus*. Microbes and Infection 2007;9:498-506.
[49] De Maere V, Vercauteren I, Geldhof P, Gevaert K, Vercruysse J, Claerebout E. Molecular analysis of astacin-like metalloproteases of *Ostertagia ostertagi*. Parasitology 2005;130:89-98.
[50] Feng J, Zhan B, Liu Y, Liu S, Williamson A, Goud G, et al. Molecular cloning and characterization of Ac-MTP-2, an astacin-like metalloprotease released by adult *Ancylostoma caninum*. Molecular and Biochemical Parasitology 2007;152:132-8.
[51] Gomez Gallego S, Loukas A, Slade RW, Neva FA, Varatharajalu R, Nutman TB, et al. Identification of an astacin-like metallo-proteinase transcript from the infective larvae of *Strongyloides stercoralis*. Parasitology International 2005;54:123-33.
[52] Williamson AL, Lustigman S, Oksov Y, Deumic V, Plieskatt J, Mendez S, et al. *Ancylostoma caninum* MTP-1, an astacin-like metalloprotease secreted by infective hookworm larvae, is involved in tissue migration. Infection and Immunity 2006;74: 961-7.
[53] Zhan B, Hotez PJ, Wang Y, Hawdon JM. A developmentally regulated metalloprotease secreted by host-stimulated *Ancylostoma caninum* third-stage infective larvae is a member of the astacin family of proteases. Molecular and Biochemical Parasitology 2002;120:291-6.
[54] Lun HM, Mak CH, Ko RC. Characterization and cloning of metallo-proteinase in the excretory/secretory products of the infective-stage larva of *Trichinella spiralis*. Parasitology Research 2003;90:27-37.
[55] Revollo JR, Grimm AA, Imai S. The NAD biosynthesis pathway mediated by nicotinamide phosphoribosyltransferase regulates Sir2 activity in mammalian cells. Journal of Biological Chemistry 2004;279:50754-63.
[56] Imai S. The N.A.D. world: a new systemic regulatory network for metabolism and aging – Sirt1, systemic NAD biosynthesis, and their importance. Cell Biochemistry and Biophysics 2009;53:65-74.
[57] Imai S. Nicotinamide phosphoribosyltransferase (Nampt): a link between NAD biology, metabolism, and diseases. Current Pharmaceutical Design 2009;15:20-8.
[58] Sah JF, Ito H, Kolli BK, Peterson DA, Sassa S, Chang KP. Genetic rescue of *Leishmania* deficiency in porphyrin biosynthesis creates mutants suitable for analysis of cellular events in uroporphyria and for photodynamic therapy. Journal of Biological Chemistry 2002;277:14902-9.
[59] Taketani S, Ishigaki M, Mizutani A, Uebayashi M, Numata M, Ohgari Y, et al. Heme synthase (ferrochelatase) catalyzes the removal of iron from heme and demetalation of metalloporphyrins. Biochemistry 2007;46:15054-61.
[60] Okeke IN, Scaletsky IC, Soars EH, Macfarlane LR, Torres AG. Molecular epidemiology of the iron utilization genes of enteroaggregative *Escherichia coli*. Journal of Clinical Microbiology 2004;42:36-44.
[61] Sancar A. Structure and function of photolyase and in vivo enzymology: 50th anniversary. Journal of Biological Chemistry 2008;283:32153-7.
[62] Wheeler JM, Thomas JH. Identification of a novel gene family involved in osmotic stress response in *Caenorhabditis elegans*. Genetics 2006;174:1327-36.
[63] Sherwood D, Stemberg P. Anchor cell invasion into the vulval epithelium in *C. elegans*. Developmental Cell 2003;5:21-35.
[64] Altun ZF, Herndon LA, Crocker C, Lints R, Hall DH. WormAtlas; 2002.
[65] Thompson DP, Geary TG. Excretion/secretion, ionic and osmotic regulation. In: Lee DL, editor. The biology of nematodes. New York: Taylor & Francis; 2002. p. 291.
[66] Hewitson JP, Grainger JR, Maizels RM. Helminth immunoregulation: the role of parasite secreted proteins in modulating host immunity. Molecular and Biochemical Parasitology 2009;167:1–11.

動物由来回虫類感染症のわが国における最近の動向

吉田彩子，長安英治，丸山治彦

宮崎大学医学部

Key Words: 食品由来寄生虫感染症，年齢性別分布，好酸球増多，生レバー

はじめに

イヌ回虫，ネコ回虫，ブタ回虫といった動物由来の回虫類による感染症は，わが国にける代表的な食品由来寄生虫病である[1]．臨床的には末梢好酸球増多を伴う肺や肝の異常陰影が主な所見で，典型的には肺や肝の陰影が移動性，あるいは消褪や出現を繰り返す．感染源はトリや牛の刺身（とくにレバー）であることが多い．診断は抗体の検出によることがほとんどで，虫体そのものが証明されることはまれといってよい[1]．

宮崎大学医学部寄生虫学では 1986 年から寄生虫病の抗体検査を実施しており，現在では multiple-dot ELISA 法による抗体スクリーニングとプレート ELISA 法による精査を組み合わせて，年間 100－200 症例の各種寄生虫病の診断に関わってきた．症例の内訳は表 1 に示す通りで，一貫して動物由来の回虫類による感染症が最も多い．しかしながら同疾患は 2004－2007 年ごろは年間 100 例ほどあったのに対し，ここ 3 年はその半数である年間 50 例を割り込んでいる．その一方で，肺吸虫症はこの間もずっと年間 30－40 例を維持しており，抗体検査が他施設で実施されるようになったり，寄生虫症例が全体として縮小しているわけではないことを示唆している．そこで今回，近年の動物由来の回虫類感染症分析し，症例数減少の原因を探った．

解析方法

症例数が年間 100 例を超えていた 2004 年と 2005 年の動物由来の回虫類感染症 203 例（04/05 年群）と，年間症例数がピーク時の半数になった 2010 年と 2011 年の 96 症例（10/11 年群）について，年齢性別分布，地理的分布，病変部位等について比較した．

Recent trends in animal-derived Ascarid infections in Japan

Ayako Yoshida, Eiji Nagayasu, Haruhiko Maruyama

Department of Infectious Diseases, Division of Parasitology, Faculty of Medicine, University of Miyazaki

論文請求先: 丸山治彦　〒889-1692 宮崎県宮崎市清武町木原 5200　宮崎大学医学部・感染症学講座・寄生虫学

表 1　宮崎大学医学部寄生虫学における寄生虫疾患診断実績

寄生虫	2001	2002	2003	2004	2005	2006	2007	2008	2009	2010	2011
イヌ回虫・ブタ回虫	68	67	77	100	103	82	101	78	49	48	48
アニサキス	6	6	6	0	4	4	6	3	2	2	3
イヌ糸状虫	6	4	4	7	1	5	1	1	0	0	0
顎口虫	13	10	11	11	0	0	6	7	9	3	4
鉤虫	6	2	3	0	1	0	1	0	1	1	1
マンソン孤虫	4	8	6	5	4	3	6	4	5	2	4
嚢虫	2	4	2	4	0	0	0	0	1	0	0
肺吸虫	37	36	32	45	30	37	46	38	38	45	35
肝蛭	1	1	8	5	6	2	3	1	1	3	2
住血吸虫	0	0	1	5	5	6	6	4	4	3	6
肝吸虫	1	3	1	1	0	0	0	0	0	1	3
糞線虫	8	21	11	11	2	1	1	2	0	2	0
回虫	3	3	4	0	1	1	1	2	0	0	0
広節・日本海裂頭条虫	0	0	2	1	0	2	0	1	0	4	2
Total	155	165	168	195	157	143	178	141	110	114	107

結果

1. 年齢性別分布

動物由来回虫類感染症の年齢分布は図 1 の通りで，04/05 年群では 30 歳代と 40－50 歳代のふたつのピークがあったが，10/11 年群では 30 歳代のピークが消えていた（図 1）．年齢分布を男女別に分けたところ，男性ではおおむね全年代で減っていたが，特に 70 歳代と 30－40 歳代の減少が顕著であった．一方女性では，20－30 歳代の若年層の症例が激減していることがわかった（図 1）．04/05 年群でみられた 20－30 歳代の女性若年層の症例内訳は，32 症例中 12 例がぶどう膜炎で眼症状の頻度が高い傾向にあった．

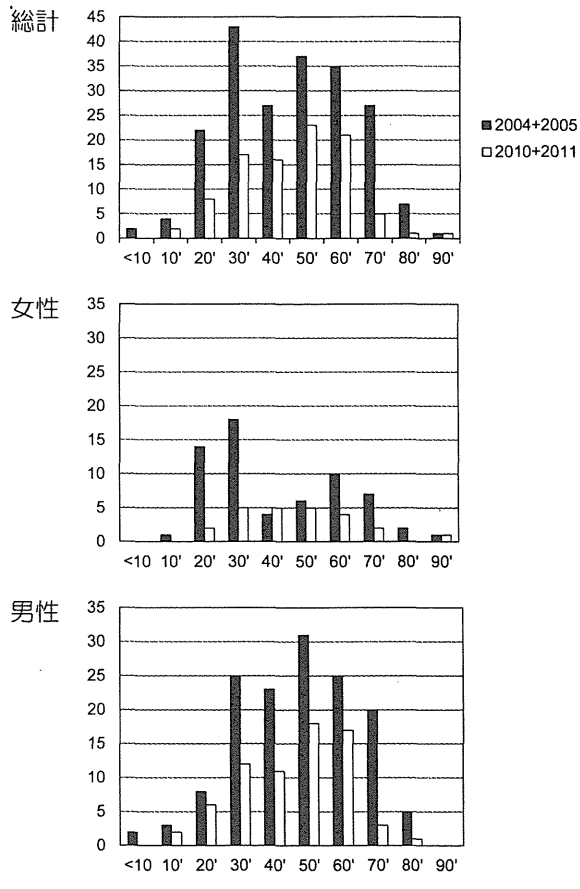

図 1 動物由来回虫類感染症の年齢性別分布
横軸は年齢，縦軸は症例数を示す

2. 地理的分布

宮崎大学のデータによれば，動物由来回虫類感染症は比較的九州地方に多い疾患である．したがって，九州地方で発生数が減少すれば全体の数も減ると予想された．患者居住地を九州・近畿・関東・その他に分けて 04/05 年群と 10/11 年群を比較したところ，どの地方でも減少は見られるもの

の，減少率では九州地方が最も大きかった（図 2）．これをさらに男女別で比較したところ，女性では各地方で約半数の減少となっていたが，男性では九州居住者が約 3 分の 1 に減少していた．一方，九州以外の男性患者はそれほど減っていないことがわかった（図 2）．つまり，動物由来回虫類感染症の減少は，女性患者の全国的な減少とともに，九州地方における男性患者の著明な減少が大きな要因であることが明らかとなった．

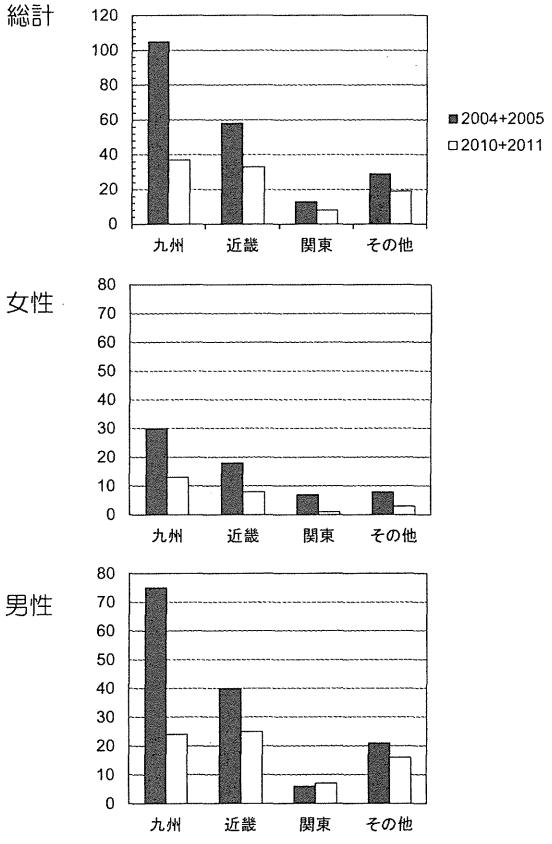

図 2　動物由来回虫類感染症の患者居住地
縦軸は症例数

3. 症状

動物由来回虫類感染症は，臨床像によって大きく 3 つに分けることができる．すなわち好酸球増多をともなう肺炎（好酸球性肺炎），視力低下などの眼症状，そして筋力低下や異常感覚などを生じる脊髄炎である．人によって体内に入った虫体が異なった病態をとる原因は明らかでないが，仮に特定の病態が減少していれば，寄生虫側または宿主側になんらかの生物学的な変化が生じた可能性も推測されうる．結果は図 3 の通りであり，男女ともに好酸球性肺炎と眼症状症例が約半数に減少し，脊髄炎症状を呈した症例の数はあまり変化がなかった．つまり，動物由来回虫類感染症という疾患全体には大きな変化はなかったことを意味している．

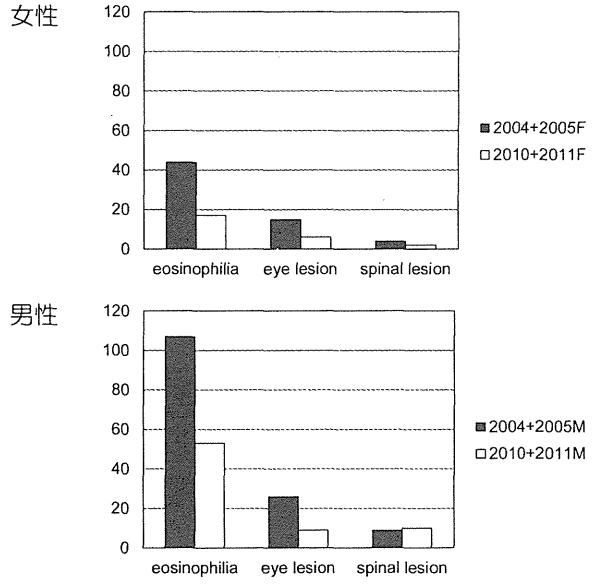

図 3　動物由来回虫類感染症
縦軸は症例数

考察

イヌ回虫症などによる動物由来回虫類感染症と肺吸虫症はどちらも代表的な食品由来の蠕虫感染症であり，わが国では中高年の男性を中心に症例が発生している．原因食品は，動物由来回虫類感染症がトリや牛の刺身，特にレバ刺しで，肺吸虫症はイノシシや淡水産のカニ（モクズガニ，サワガニ）である．どちらの疾患も末梢血の好酸球増多が診断のきっかけとなることが多い．トキソカラ眼症やトキソカラ脊髄炎では末梢の好酸

球増多がなくても，臨床症状から感染が疑われ得る．

宮崎大学医学部寄生虫学では 1986 年から寄生虫病の抗体検査を受託しており，multiple-dot ELISA 法による抗体スクリーニングとプレート ELISA 法による精査を組み合わせて，年間 100－200 症例の各種寄生虫病の診断に関わってきた．動物由来回虫類感染症と肺吸虫症は，一貫して症例数の上位にあるが，2001 年以降の各疾患における症例数を見てみると，肺吸虫症は年間 30－40 症例でほぼ変化していないのに対し，かつて年間 100 例を上回ることもあった動物由来回虫類感染症は近年では年間 50 例を切っている．

症例分析の結果，動物由来回虫類感染症が大きく減少したのは，女性患者の全国的な減少と九州地方における男性患者の著明な減少によることが明らかになった．その理由としては，トリや牛におけるトキソカラ等寄生虫感染の減少か，あるいはトリや牛の刺身，特にレバ刺しの摂取機会の減少が理論上は考えられる．しかしながら，依然として首都圏の砂場でもトキソカラの虫卵が検出されていることから [2]，トリや牛におけるトキソカラ等の回虫類感染がここ数年というスパンで大きく減少したということは考えにくく，摂食行動の変化の方が可能性としては高いように考えられる．

トリや牛のレバ刺しによる食中毒は近年大きな社会的問題となっており，カンピロバクターによる腸炎，病原性大腸菌による出血性大腸炎，サルモネラ感染症などが大きく報道されている．とくに腸管出血性大腸菌感染症は毎年死者を出しており，生肉や生レバーに存在する危険性は社会的に認知されてきた．厚生労働省も牛レバーについては安全な食品と汚染食品を区別する有効な手段がないとして，生食レバーの提供禁止を平成 24 年 7 月 1 日から実施することに踏み切った [3]．生レバー摂取動向に関する信頼できるデータは存在しないが，今後提供禁止が食行動にどのような影響を与えるか注目に値する．

動物由来回虫類感染症は，病原性大腸菌のように致命的であることはないが，眼症状や脊髄炎症状を引き越すことがある．また，治療はアルベンダゾールを 4－6 週服用し続ける必要があり時に薬剤性肝障害を引き越すことがある 4)．いずれにせよ感染しないに越したことはないので，臨床寄生虫学に関わるのもとしては，牛，トリ，その他動物種に関わらず，生の獣肉・レバーの摂取は控えるように訴えていくべきであろう．

文　献

1) Akao, N. *et al.* (2007) : Toxocariasis in Japan. Parasitol Int. 56, 87-93.

2) Macuhova, K. *et al.* (2010) : Loop-mediated isothermal amplification assay for detection and discrimination of *Toxocara canis* and *Toxocara cati* eggs directly from sand samples. J Parasitol. 96, 1224-1227.

3) 厚生労働省医薬食品局食品安全部長 (2012) : 食品，添加物等の規格基準の一部を改正する件について．平成 24 年厚生労働省告示第 404 号．平成 24 年 6 月 25 日．

4) Yoshikawa, M. *et al.* (2011) : Lessons from eight cases of adult pulmonary toxocariasis: abridged republication. Respirology. Aug; 16: 1014-5. doi: 10.1111/j.1440-1843.2011.02000.x.